Journal of Computational Physics 377 (2019) 117–141

Contents lists available at ScienceDirect

Journal of Computational Physics

www.elsevier.com/locate/jcp

Maximum-principle-preserving third-order local discontinuous Galerkin method for convection-diffusion equations on overlapping meshes ☆

Jie Du [a], Yang Yang [b,*]

[a] Yau Mathematical Sciences Center, Tsinghua University, Beijing, China
[b] Department of Mathematical Sciences, Michigan Technological University, Houghton, MI 49931, United States of America

ARTICLE INFO

Article history:
Received 11 February 2018
Received in revised form 28 September 2018
Accepted 23 October 2018
Available online 25 October 2018

Keywords:
Convection-diffusion equations
Maximum-principle-preserving
Local discontinuous Galerkin method
Overlapping mesh

ABSTRACT

Local discontinuous Galerkin (LDG) methods are popular for convection-diffusion equations. In LDG methods, we introduce an auxiliary variable p to represent the derivative of the primary variable u, and solve them on the same mesh. It is well known that the maximum-principle-preserving (MPP) LDG method is only available up to second-order accuracy. Recently, we introduced a new algorithm, and solve u and p on different meshes, and obtained stability and optimal error estimates. In this paper, we will continue this approach and construct MPP third-order LDG methods for convection-diffusion equations on overlapping meshes. The new algorithm is more flexible and does not increase any computational cost. Numerical evidence will be given to demonstrate the accuracy and good performance of the third-order MPP LDG method.

1. Introduction

In this paper, we aim to construct maximum-principle-preserving (MPP) third-order local discontinuous Galerkin (LDG) schemes for solving the following convection-diffusion equation

$$u_t + f(u)_x = b(u)_{xx}, \tag{1.1}$$

or equivalently

$$u_t + f(u)_x = (a^2(u)u_x)_x, \tag{1.2}$$

as well as their two-dimensional versions, where $a^2(u) = b'(u) \geq 0$. We also assume that $a(u) \geq 0$ and periodic boundary conditions. The initial condition is given as $u(x, 0) = u_0(x)$. It is well known that the exact solution satisfies a strict maximum-principle, i.e.,

$$u(x, t) \in [m, M], \quad \forall x \in \mathbb{R}, \quad \forall t \geq 0,$$

☆ Supported by the NSF grant DMS-1818467.
* Corresponding author.
E-mail addresses: jdu@mail.tsinghua.edu.cn (J. Du), yyang7@mtu.edu (Y. Yang).

https://doi.org/10.1016/j.jcp.2018.10.034
0021-9991/

where $m = \min_x u_0(x)$ and $M = \max_x u_0(x)$. In particular, if $m = 0$, the exact solution will maintain non-negative for all time, resulting in the positivity-preserving (PP) property.

The discontinuous Galerkin (DG) method was first introduced in 1973 by Reed and Hill [22] in the framework of neutron linear transport. Subsequently, Cockburn et al. developed Runge–Kutta discontinuous Galerkin (RKDG) methods for hyperbolic conservation laws in a series of papers [6,4,5,7]. In [8], Cockburn and Shu introduced the LDG method to solve the convection-diffusion equations. Their idea was motivated by Bassi and Rebay [1], where the compressible Navier–Stokes equations were successfully solved. Recently, in [27], genuinely MPP high-order DG schemes for scalar conservation laws and two-dimensional incompressible flows in vorticity-streamfunction formulation have been constructed. Subsequently, PP high-order DG schemes for compressible Euler equations were given in [28,29]. Later, the technique was applied to other hyperbolic systems, such as pressureless Euler equations [26], extended MHD equations [31], relativistic hydrodynamics [21], etc., and the L^1 stability was demonstrated. For parabolic equations, the extension was given in [30], where second-order MPP discontinuous Galerkin methods were demonstrated, and the construction of high-order schemes seem to be not straightforward. Later another approach based on the flux limiter were discussed in [25,15]. In [2], the third-order MPP direct DG method was introduced. However, the scheme was not easy to implement and we need to add two penalty terms. In this paper, we will introduce the modified LDG method on overlapping meshes and construct MPP third-order LDG methods.

As in traditional LDG methods, we introduce an auxiliary variable p to represent $a(u)u_x$ and thus can rewrite (1.2) into the following system of first order equations

$$\begin{cases} u_t + f(u)_x = (a(u)p)_x, \\ p = A(u)_x, \end{cases} \tag{1.3}$$

where $A(u) = \int_0^u a(\tau)d\tau$. Usually, u and p are solved on the same mesh. In [11], we introduced a new algorithm and solve u and p on the primitive and dual meshes, respectively, where the dual mesh is generated from the primitive one. There are several advantages of the new algorithm.

1. The fluxes for the convection terms are easy to construct.
   It is well known that due to the discontinuity of the numerical approximations across the cell interfaces, we need to introduce the numerical fluxes. For convection-diffusion equations, the fluxes for the diffusion terms seem to be easy to construct and in most cases we can simply choose the alternating ones [8]. However, the fluxes for the convection terms are not easy to construct. Especially for some convection-diffusion systems such as the chemotaxis model [17,20] and miscible displacements in porous media [9,10], where the convection terms are the products of one of the primary variables and the derivatives of another primary variable. Due to the discontinuity nature of the DG methods, most of the well established numerical fluxes, such as the upwind fluxes, cannot be applied, since the coefficients of the convection terms turn out to be discontinuous after the spatial discretization. It is well known that hyperbolic equations with discontinuous coefficients are in general not well-posed [12,16]. Therefore, the DG schemes may not be stable when applied to those model equations. To make the numerical solutions to be physically relevant, we have to add very large penalty terms which depend on the numerical approximations of the derivatives of the primary variables [18,14]. With the new algorithm, the derivatives, solving on the dual mesh, are continuous across the cell interfaces on the primitive mesh, hence the upwind fluxes can be applied.
2. The new algorithm is more flexible without increasing the computational cost.
   It is well known that to avoid the numerical fluxes, some modification of DG methods have been introduced, such as the Central DG (CDG) methods [19] and Staggered DG (SDG) methods [3]. For CDG methods, we have to solve each equation in (1.3) on both the primitive and dual meshes, which doubles the computational cost. In our new method, we solve u on the primitive mesh and p on the dual mesh, respectively. Therefore, the computational cost is exactly the same as the original LDG method. Moreover, different from the SDG methods, we do not require any continuity conditions across the cell interfaces for u on the primitive cells or p on the dual meshes. Therefore, the new LDG method is more flexible and it is very convenient to apply limiters.
3. Most importantly, we can construct third-order MPP schemes.
   In [30], the authors demonstrated that the original MPP LDG methods are only available up to second-order accuracy. In the new algorithm, we add a mild penalty, which does not depend on the numerical approximations, in the equation of u, and construct third-order MPP schemes. Since the dual mesh can be moved arbitrarily, we will show that if the dual mesh agree with the primitive mesh, the penalty coefficient turns out to be infinity. Therefore, our algorithm does not violate the results given in [30]. Finally, the new algorithm is stable and easy to understand and construct [11]. It is able to be generated to higher order schemes. For convection-diffusion equations, the rates of accuracy are optimal. However, numerical experiments demonstrate a suboptimal rate of convergence if odd order polynomials were applied to pure diffusion equations. In [11], we have introduced a couple of ways to recover optimal convergence rates. Therefore, we will not discuss the error estimates in this paper, and focus on the MPP technique only.

The organization of this paper is as follows. In Section 2, we construct the new LDG scheme for one dimensional nonlinear convection-diffusion equations on overlapping meshes. In Section 3, we introduced the MPP technique in one space

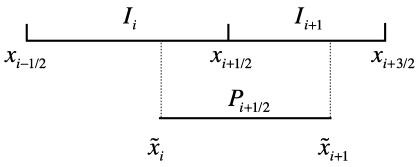

Fig. 2.1. Overlapping meshes.

dimension. Generations of the new LDG scheme and the MPP technique to two space dimensions will be given in Section 4. Numerical experiments in one and two space dimensions will be given in Section 5 to demonstrate the accuracy and good performance of the new third-order MPP LDG scheme. Finally, we will end in Section 6 with concluding remarks and remarks for future works.

2. LDG scheme on overlapping meshes in one space dimension

In this section, we first illustrate the generation of overlapping meshes in one space dimension as well as some notations in Section 2.1, and then show how to construct LDG methods on the generated overlapping meshes in Section 2.2. For simplicity, we consider the periodic boundary condition. The analyses for other boundary conditions will be discussed in the future.

2.1. Overlapping meshes

Fig. 2.1 is an illustration of the overlapping meshes. The mesh on the top in this figure is the primitive mesh on which the original variable u is solved, while the one in the bottom is the dual mesh on which the auxiliary variable p is solved.

We first show how to define the primitive mesh. It is just a regular decomposition of the computational domain $[0, 1]$, which can be non-uniform. We denote the i-th cell as

$$I_i = [x_{i-\frac{1}{2}}, x_{i+\frac{1}{2}}], \quad i = 1, \cdots, N_x.$$

The cell length and the cell center of I_i are denoted as

$$\triangle x_i = x_{i+\frac{1}{2}} - x_{i-\frac{1}{2}}, \qquad x_i = \frac{x_{i-\frac{1}{2}} + x_{i+\frac{1}{2}}}{2},$$

respectively. Based on the primitive mesh, we move each cell center within the corresponding cell to obtain a new mesh called the P-mesh, which is used to solve the auxiliary variable p, i.e. in each cell I_i, we choose a point $\tilde{x}_i$ given as

$$\tilde{x}_i = x_i + \frac{\triangle x_i}{2}\xi_{i0}, \qquad \xi_{i0} \in [-1, 1], \quad i = 1, \cdots, N_x. \tag{2.1}$$

For simplicity, we consider ξ_{i0} to be a constant independent of i and denoted as $\xi_0 \in [-1, 1]$. Note that here the subscript 0 is used to describe a constant but not the index of cell. It is easy to check $\tilde{x}_i \in [x_{i-\frac{1}{2}}, x_{i+\frac{1}{2}}]$. The $(i-\frac{1}{2})$-th cell of the dual mesh is defined as

$$P_{i-\frac{1}{2}} = [\tilde{x}_{i-1}, \tilde{x}_i], \quad i = 1, \cdots, N_x,$$

where we denote $\tilde{x}_0 = \tilde{x}_{N_x} - 1$. We further denote the cell length and the cell center of $P_{i-\frac{1}{2}}$ as

$$\triangle \tilde{x}_{i-\frac{1}{2}} = \tilde{x}_i - \tilde{x}_{i-1}, \qquad \tilde{x}_{i-\frac{1}{2}} = \frac{\tilde{x}_{i-1} + \tilde{x}_i}{2},$$

respectively. Notice that when $\xi_0 = 0$, we have $\tilde{x}_i = x_i$ and $P_{i+\frac{1}{2}} = [x_i, x_{i+1}]$. In this case, the cell interfaces of the dual mesh are exactly the cell centers of the primitive mesh. Due to the periodic boundary condition, we can also define $P_{\frac{1}{2}} = [0, \tilde{x}_1] \cup [\tilde{x}_{N_x}, 1]$. Therefore, we regard a function on $P_{\frac{1}{2}}$ as a function on $[\tilde{x}_0, \tilde{x}_1]$. We define the dual mesh to be the P-mesh which consists of all these P cells. This kind of mesh is the most commonly used overlapping mesh, such as in the CDG method [19]. When $\xi_0 = -1$, we have $\tilde{x}_i = x_{i-\frac{1}{2}}$ and hence the P-mesh is the same as the primitive mesh.

2.2. LDG method on overlapping meshes

Base on the previous defined overlapping meshes, we are ready to construct the LDG method for (1.3). The finite element space on each mesh consists of piecewise polynomials:

$$V_h := \{u_h : u_h|_{I_i} \in P^k(I_i),\ i = 1, \cdots, N_x\},$$
$$P_h := \{p_h : p_h|_{P_{i-\frac{1}{2}}} \in P^k(P_{i-\frac{1}{2}}),\ i = 1, \cdots, N_x\},$$

where $P^k(I_i)$ and $P^k(P_{i-\frac{1}{2}})$ are the sets of all polynomials of degree up to k defined on the cell I_i and $P_{i-\frac{1}{2}}$, respectively.

We multiply the first equation in (1.3) with a test function $v \in V_h$ and integrate this equation on the primitive mesh. Similarly, we multiply the second equation with a test function $w \in P_h$ and integrate it on the dual mesh. By using integration by parts, our new LDG method on overlapping meshes is defined as follows: to find $(u_h, p_h) \in V_h \times P_h$, such that for any test functions $(v, w) \in V_h \times P_h$ and any i, we have

$$\int_{I_i} (u_h)_t v dx = -\int_{I_i} (a(u_h)p_h - f(u_h))\, v_x dx + (\hat{a}_{i+\frac{1}{2}}\hat{p}_{i+\frac{1}{2}} - \hat{f}_{i+\frac{1}{2}})v^-_{i+\frac{1}{2}} - (\hat{a}_{i-\frac{1}{2}}\hat{p}_{i-\frac{1}{2}} - \hat{f}_{i-\frac{1}{2}})v^+_{i-\frac{1}{2}}, \tag{2.2}$$

$$\int_{P_{i-\frac{1}{2}}} p_h w dx = -\int_{P_{i-\frac{1}{2}}} A(u_h)w_x dx + A(u_h(\tilde{x}_i))w^-_i - A(u_h(\tilde{x}_{i-1}))w^+_{i-1}, \tag{2.3}$$

where $v^-_{i+\frac{1}{2}} = v^-(x_{i+\frac{1}{2}})$ and $w^-_i = w^-(\tilde{x}_i)$. Likewise for $v^+_{i-\frac{1}{2}}$ and w^+_{i-1}. For simplicity, we denote $v^-_{\frac{1}{2}} = v^-_{N_x+\frac{1}{2}}$ and $v^+_{N_x+\frac{1}{2}} = v^+_{\frac{1}{2}}$. The numerical flux $\hat{a}$ at the point $x_{i+\frac{1}{2}}$ is taken as

$$\hat{a}_{i+\frac{1}{2}} = \frac{[A(u_h)]_{i+\frac{1}{2}}}{[u_h]_{i+\frac{1}{2}}},$$

where $[s]_{i+\frac{1}{2}} := s^+_{i+\frac{1}{2}} - s^-_{i+\frac{1}{2}}$ denotes the jump of a function s across the cell interface $x = x_{i+\frac{1}{2}}$. Similarly, we can also denote the jump of w across $x = \tilde{x}_i$ on the P-mesh as $[w]_i = w^+_i - w^-_i$. For simplicity, if $[u_h] = 0$, we define $\hat{a} = a(u_h)$. The flux for the convection term $\hat{f}_{i+\frac{1}{2}} = \hat{f}(u^-_{i+\frac{1}{2}}, u^+_{i+\frac{1}{2}})$ is the usual monotone flux used in the traditional DG methods. More details for the suitable numerical fluxes can be found in [27]. p_h is defined as a piecewise polynomial on the dual mesh and it is continuous at the cell interfaces of the primitive mesh, hence $p_h(x_{i+\frac{1}{2}})$ is well-defined. We take

$$\hat{p}_{i+\frac{1}{2}} = p_h(x_{i+\frac{1}{2}}) + \frac{\alpha_{i+\frac{1}{2}}}{\triangle\tilde{x}_{i+\frac{1}{2}}}[A(u_h)]_{i+\frac{1}{2}}, \tag{2.4}$$

where the parameter $\alpha_{i+\frac{1}{2}}$ is chosen by the MPP technique.

3. MPP third-order LDG scheme in one space dimension

In this section, we proceed to demonstrate the MPP technique and consider the third-order scheme only, i.e. $k = 2$.

3.1. Analysis for the spacial discretization

In this subsection, we apply Euler forward time discretization and analyze the spacial discretization. We use u^n_h as the numerical solution at time level n and use $\bar{u}^n_i$ to denote the cell average of u^n_h on I_i. For simplicity, if we consider the numerical approximation at time level n, then the superscript will be omitted. Taking $v = 1$ in (2.2), we obtain the equation satisfied by the numerical cell average $\bar{u}_i$

$$\bar{u}^{n+1}_i = \left(\frac{1}{2}\bar{u}^n_i - \frac{\triangle t}{\triangle x_i}(\hat{f}_{i+\frac{1}{2}} - \hat{f}_{i-\frac{1}{2}})\right) + \left(\frac{1}{2}\bar{u}^n_i + \frac{\triangle t}{\triangle x_i}(\hat{a}_{i+\frac{1}{2}}\hat{p}_{i+\frac{1}{2}} - \hat{a}_{i-\frac{1}{2}}\hat{p}_{i-\frac{1}{2}})\right) := \frac{1}{2}C_i + \frac{1}{2}D_i, \tag{3.1}$$

where

$$C_i = \bar{u}^n_i - \frac{2\triangle t}{\triangle x_i}(\hat{f}_{i+\frac{1}{2}} - \hat{f}_{i-\frac{1}{2}}), \quad \text{and} \quad D_i = \bar{u}^n_i + \frac{2\triangle t}{\triangle x_i}(\hat{a}_{i+\frac{1}{2}}\hat{p}_{i+\frac{1}{2}} - \hat{a}_{i-\frac{1}{2}}\hat{p}_{i-\frac{1}{2}}) \tag{3.2}$$

are the convection and diffusion terms, respectively. In this section, we assume $u^n_h \in [m, M]$ and aim to find sufficient conditions to make $C_i, D_i \in [m, M]$, and thus $\bar{u}^{n+1}_i \in [m, M]$. The technique for C_i has been discussed in [27] and we recall the result for the frequently used Lax–Friedrichs flux here.

Lemma 3.1. *Consider the global Lax–Friedrichs flux*

$$\hat{f}_{i+\frac{1}{2}} = \frac{1}{2}[f(u^-_{i+\frac{1}{2}}) + f(u^+_{i+\frac{1}{2}}) - a(u^+_{i+\frac{1}{2}} - u^-_{i+\frac{1}{2}})], \qquad a = \max_u |f'(u)|,$$

where the maximum is taken over the whole region where u vary. Suppose $m \le u_h^n \le M$, *then we have* $m \le C_i \le M$, *under the condition*

$$\Delta t \le \frac{\min_\beta w_\beta}{4a} \min_i \Delta x_i, \tag{3.3}$$

where $w'_\beta s$ *are the quadrature weights for the 3-point Legendre Gauss–Lobatto quadrature for the interval* $[-1, 1]$.

The rest of this section will focus on the MPP technique for the diffusion term D_i. We divide the whole algorithm into five steps and demonstrate the implementation of the technique in the end.

Step 1: Computation of $p_h(x_{i+\frac{1}{2}})$ and $p_h(x_{i-\frac{1}{2}})$

We need to solve $p_h(x_{i+\frac{1}{2}})$ and $p_h(x_{i-\frac{1}{2}})$ by (2.3) and thus can rewrite D_i as a function of u_h^n. For simplicity, we map $x \in P_{i+\frac{1}{2}} = [\tilde{x}_i, \tilde{x}_{i+1}]$ onto the standard element $\xi \in [-1, 1]$ as

$$x = \tilde{x}_{i+\frac{1}{2}} + \frac{\triangle\tilde{x}_{i+\frac{1}{2}}}{2}\xi, \qquad \xi = \frac{2x - 2\tilde{x}_{i+\frac{1}{2}}}{\triangle\tilde{x}_{i+\frac{1}{2}}} := \xi^{i+\frac{1}{2}}(x), \tag{3.4}$$

where in the second equation we can view ξ as a function of x and denote this function as $\xi^{i+\frac{1}{2}}(x)$. Moreover, we denote Legendre polynomial functions on $[-1, 1]$ as

$$L_0 = 1, \qquad L_1(\xi) = \xi, \qquad L_2(\xi) = \frac{1}{2}(3\xi^2 - 1), \tag{3.5}$$

and represent $p_h|_{P_{i+\frac{1}{2}}}$ on the standard element as

$$p_h(x(\xi)) = p_0(\xi) = a_0 L_0 + a_1 L_1(\xi) + a_2 L_2(\xi), \qquad \xi \in [-1, 1].$$

Here the subscript in p_0 is not the index of cell. We just use it to describe a function defined on $[-1, 1]$. Notice that $x_{i+\frac{1}{2}} \in [\tilde{x}_i, \tilde{x}_{i+1}]$, by simple computations, we know that

$$x_{i+\frac{1}{2}} = \tilde{x}_{i+\frac{1}{2}} + \frac{\triangle\tilde{x}_{i+\frac{1}{2}}}{2}\xi_{i+\frac{1}{2}},$$

where

$$\xi_{i+\frac{1}{2}} = \frac{-\xi_0(dx_{i+\frac{1}{2}} + 1) + (dx_{i+\frac{1}{2}} - 1)}{\xi_0(1 - dx_{i+\frac{1}{2}}) + (dx_{i+\frac{1}{2}} + 1)} \in [-1, 1], \tag{3.6}$$

and $dx_{i+\frac{1}{2}} = \frac{\triangle x_i}{\triangle x_{i+1}}$. Hence, we have

$$p_h(x_{i+\frac{1}{2}}) = p_0(\xi_{i+\frac{1}{2}}) = a_0 + a_1\xi_{i+\frac{1}{2}} + \frac{a_2}{2}(3\xi^2_{i+\frac{1}{2}} - 1). \tag{3.7}$$

By using the orthogonal property of Legendre polynomial basis functions, we can get

$$a_0 = \frac{1}{2}\int_{-1}^{1} p_0 L_0 d\xi, \qquad a_1 = \frac{3}{2}\int_{-1}^{1} p_0 L_1 d\xi, \qquad a_2 = \frac{5}{2}\int_{-1}^{1} p_0 L_2 d\xi. \tag{3.8}$$

Substituting (3.8) into the (3.7), we obtain

$$p_h(x_{i+\frac{1}{2}}) = \frac{1}{2}\int_{-1}^{1} p_0(\xi) s^{i+\frac{1}{2}}(\xi) d\xi, \tag{3.9}$$

where $s^{i+\frac{1}{2}}$ is a function of ξ defined as

$$s^{i+\frac{1}{2}}(\xi) = 1 + 3\xi_{i+\frac{1}{2}}\xi + \frac{5}{4}(3\xi^2_{i+\frac{1}{2}} - 1)(3\xi^2 - 1), \qquad \xi \in [-1, 1]. \tag{3.10}$$

We then revert back to the physical element $P_{i+\frac{1}{2}}$. By using (2.3), we get

$$
\begin{aligned}
p_h(x_{i+\frac{1}{2}}) &= \frac{1}{2}\int_{-1}^{1} p_0(\xi)s^{i+\frac{1}{2}}(\xi)d\xi = \frac{1}{\triangle\tilde{x}_{i+\frac{1}{2}}}\int_{P_{i+\frac{1}{2}}} p_h(x)s^{i+\frac{1}{2}}\left(\xi^{i+\frac{1}{2}}(x)\right)dx \\
&= \frac{1}{\triangle\tilde{x}_{i+\frac{1}{2}}}\left[-\int_{\tilde{x}_i}^{\tilde{x}_{i+1}} A(u_h)s^{i+\frac{1}{2}}\left(\xi^{i+\frac{1}{2}}(x)\right)_x dx + A(u_h(\tilde{x}_{i+1}))s^{i+\frac{1}{2}}(1) - A(u_h(\tilde{x}_i))s^{i+\frac{1}{2}}(-1)\right] \\
&= \frac{1}{\triangle\tilde{x}_{i+\frac{1}{2}}}\left[-\int_{\tilde{x}_i}^{x_{i+\frac{1}{2}}} A(u_h)s^{i+\frac{1}{2}}\left(\xi^{i+\frac{1}{2}}(x)\right)_x dx - A(u_h(\tilde{x}_i))s^{i+\frac{1}{2}}(-1)\right] \\
&+ \frac{1}{\triangle\tilde{x}_{i+\frac{1}{2}}}\left[\int_{x_{i+\frac{1}{2}}}^{\tilde{x}_{i+1}} A(u_h)_x s^{i+\frac{1}{2}}\left(\xi^{i+\frac{1}{2}}(x)\right)dx + A(u_h^+(x_{i+\frac{1}{2}}))s^{i+\frac{1}{2}}(\xi_{i+\frac{1}{2}})\right],
\end{aligned}
\tag{3.11}
$$

where the integration by part is used in the last step. Similarly, we can compute $p_h(x_{i-\frac{1}{2}})$ as

$$
\begin{aligned}
p_h(x_{i-\frac{1}{2}}) &= \frac{1}{\triangle\tilde{x}_{i-\frac{1}{2}}}\left[\int_{\tilde{x}_{i-1}}^{x_{i-\frac{1}{2}}} A(u_h)_x s^{i-\frac{1}{2}}\left(\xi^{i-\frac{1}{2}}(x)\right)dx - A(u_h^-(x_{i-\frac{1}{2}}))s^{i-\frac{1}{2}}(\xi_{i-\frac{1}{2}})\right] \\
&+ \frac{1}{\triangle\tilde{x}_{i-\frac{1}{2}}}\left[-\int_{x_{i-\frac{1}{2}}}^{\tilde{x}_i} A(u_h)s^{i-\frac{1}{2}}\left(\xi^{i-\frac{1}{2}}(x)\right)_x dx + A(u_h(\tilde{x}_i))s^{i-\frac{1}{2}}(1)\right].
\end{aligned}
\tag{3.12}
$$

Step 2: Decomposition of D_i

We consider the decomposition of D_i. Substituting (3.11) and (3.12) into (3.2), we can decompose D_i as

$$
\begin{aligned}
D_i &= \bar{u}_i^n + \frac{2\hat{a}_{i+\frac{1}{2}}\triangle t}{\triangle x_i}\left[p_h(x_{i+\frac{1}{2}}) + \frac{\alpha_{i+\frac{1}{2}}}{\triangle\tilde{x}_{i+\frac{1}{2}}}[A]_{i+\frac{1}{2}}\right] - \frac{2\hat{a}_{i-\frac{1}{2}}\triangle t}{\triangle x_i}\left[p_h(x_{i-\frac{1}{2}}) + \frac{\alpha_{i-\frac{1}{2}}}{\triangle\tilde{x}_{i-\frac{1}{2}}}[A]_{i-\frac{1}{2}}\right] \\
&= \bar{u}_i^n + \frac{2\triangle t}{\triangle x_i}U_i + \frac{2\triangle t\hat{a}_{i+\frac{1}{2}}}{\triangle x_i\triangle\tilde{x}_{i+\frac{1}{2}}}U_{i+1} + \frac{2\triangle t\hat{a}_{i-\frac{1}{2}}}{\triangle x_i\triangle\tilde{x}_{i-\frac{1}{2}}}U_{i-1},
\end{aligned}
\tag{3.13}
$$

where

$$
\begin{aligned}
U_i &= \frac{\hat{a}_{i+\frac{1}{2}}}{\triangle\tilde{x}_{i+\frac{1}{2}}}\left[-\int_{\tilde{x}_i}^{x_{i+\frac{1}{2}}} A(u_h)s^{i+\frac{1}{2}}\left(\xi^{i+\frac{1}{2}}(x)\right)_x dx - A(u_h(\tilde{x}_i))s^{i+\frac{1}{2}}(-1) - \alpha_{i+\frac{1}{2}}A(u_h^-(x_{i+\frac{1}{2}}))\right] \\
&- \frac{\hat{a}_{i-\frac{1}{2}}}{\triangle\tilde{x}_{i-\frac{1}{2}}}\left[-\int_{x_{i-\frac{1}{2}}}^{\tilde{x}_i} A(u_h)s^{i-\frac{1}{2}}\left(\xi^{i-\frac{1}{2}}(x)\right)_x dx + A(u_h(\tilde{x}_i))s^{i-\frac{1}{2}}(1) + \alpha_{i-\frac{1}{2}}A(u_h^+(x_{i-\frac{1}{2}}))\right],
\end{aligned}
\tag{3.14}
$$

$$
U_{i+1} = \int_{x_{i+\frac{1}{2}}}^{\tilde{x}_{i+1}} A(u_h)_x s^{i+\frac{1}{2}}\left(\xi^{i+\frac{1}{2}}(x)\right)dx + A(u_h^+(x_{i+\frac{1}{2}}))\left[s^{i+\frac{1}{2}}(\xi_{i+\frac{1}{2}}) + \alpha_{i+\frac{1}{2}}\right],
\tag{3.15}
$$

$$
U_{i-1} = -\int_{\tilde{x}_{i-1}}^{x_{i-\frac{1}{2}}} A(u_h)_x s^{i-\frac{1}{2}}\left(\xi^{i-\frac{1}{2}}(x)\right)dx + A(u_h^-(x_{i-\frac{1}{2}}))\left[s^{i-\frac{1}{2}}(\xi_{i-\frac{1}{2}}) + \alpha_{i-\frac{1}{2}}\right].
\tag{3.16}
$$

Step 3: PP technique for linear case

Now we proceed to discuss the PP technique for linear diffusion terms, i.e. $A(u) = u$, $m = 0$ and $M = \infty$. Then (3.14)–(3.16) can be written as

$$U_i = \frac{1}{\triangle\tilde{x}_{i+\frac{1}{2}}}\left[-\int_{\tilde{x}_i}^{x_{i+\frac{1}{2}}} u_h s^{i+\frac{1}{2}}\left(\xi^{i+\frac{1}{2}}(x)\right)_x dx - u_h(\tilde{x}_i)s^{i+\frac{1}{2}}(-1) - \alpha_{i+\frac{1}{2}}u_h^-(x_{i+\frac{1}{2}})\right]$$
$$- \frac{1}{\triangle\tilde{x}_{i-\frac{1}{2}}}\left[-\int_{x_{i-\frac{1}{2}}}^{\tilde{x}_i} u_h s^{i-\frac{1}{2}}\left(\xi^{i-\frac{1}{2}}(x)\right)_x dx + u_h(\tilde{x}_i)s^{i-\frac{1}{2}}(1) + \alpha_{i-\frac{1}{2}}u_h^+(x_{i-\frac{1}{2}})\right], \tag{3.17}$$

$$U_{i+1} = \int_{x_{i+\frac{1}{2}}}^{\tilde{x}_{i+1}} (u_h)_x s^{i+\frac{1}{2}}\left(\xi^{i+\frac{1}{2}}(x)\right)dx + u_h^+(x_{i+\frac{1}{2}})\left[s^{i+\frac{1}{2}}(\xi_{i+\frac{1}{2}}) + \alpha_{i+\frac{1}{2}}\right], \tag{3.18}$$

$$U_{i-1} = -\int_{\tilde{x}_{i-1}}^{x_{i-\frac{1}{2}}} (u_h)_x s^{i-\frac{1}{2}}\left(\xi^{i-\frac{1}{2}}(x)\right)dx + u_h^-(x_{i-\frac{1}{2}})\left[s^{i-\frac{1}{2}}(\xi_{i-\frac{1}{2}}) + \alpha_{i-\frac{1}{2}}\right]. \tag{3.19}$$

We will consider U_i first and the result is given below.

Lemma 3.2. *Suppose $u_h \geq 0$ in I_i, where I_i is a certain element. Then $\bar{u}_i + \frac{2\triangle t}{\triangle x_i}U_i \geq 0$ under the condition*

$$\triangle t \leq \frac{\triangle x^2}{12\left[\max_i h(|\xi_{i+\frac{1}{2}}|) + 3\ell(\xi_0) + 3\max_i \alpha_{i+\frac{1}{2}}\right]}, \tag{3.20}$$

where $\triangle x = \min_i\{\triangle\tilde{x}_{i+\frac{1}{2}}, \triangle x_i\}$,

$$h(\xi) = \begin{cases} \xi\left(1 + \frac{5}{2}(3\xi^2 - 1)\right), & \text{if} \quad 3\xi^2 - 1 \geq 0 \\ \xi - \frac{5}{2}(3\xi^2 - 1), & \text{if} \quad 3\xi^2 - 1 < 0 \end{cases} \tag{3.21}$$

and

$$\ell(\xi) = \max\left\{\frac{5}{2}(3\xi^2 - 1) + 3|\xi| + 1,\ 1 - \frac{3\xi^2}{5(3\xi^2 - 1)} - \frac{5}{4}(3\xi^2 - 1)\right\}. \tag{3.22}$$

Proof. When $U_i \geq 0$, it is obvious that $\bar{u}_i^n + \frac{\triangle t}{\triangle x_i}U_i \geq 0$. Hence we only need to consider the case with $U_i < 0$. In this case, we need to require $\triangle t \leq \frac{\bar{u}_i^n}{-U_i/\triangle x_i}$. Next, we try to find an upper bound of $-\frac{U_i}{\triangle x_i}$.

$$-\frac{U_i}{\triangle x_i} = \frac{1}{\triangle x_i \triangle\tilde{x}_{i+\frac{1}{2}}}\int_{\tilde{x}_i}^{x_{i+\frac{1}{2}}} u_h s^{i+\frac{1}{2}}\left(\xi^{i+\frac{1}{2}}(x)\right)_x dx - \frac{1}{\triangle x_i \triangle\tilde{x}_{i-\frac{1}{2}}}\int_{x_{i-\frac{1}{2}}}^{\tilde{x}_i} u_h s^{i-\frac{1}{2}}\left(\xi^{i-\frac{1}{2}}(x)\right)_x dx$$
$$+ \left(\frac{s^{i+\frac{1}{2}}(-1)}{\triangle x_i \triangle\tilde{x}_{i+\frac{1}{2}}} + \frac{s^{i-\frac{1}{2}}(1)}{\triangle x_i \triangle\tilde{x}_{i-\frac{1}{2}}}\right)u_h(\tilde{x}_i) + \frac{\alpha_{i+\frac{1}{2}}}{\triangle x_i \triangle\tilde{x}_{i+\frac{1}{2}}}u_h^-(x_{i+\frac{1}{2}}) + \frac{\alpha_{i-\frac{1}{2}}}{\triangle x_i \triangle\tilde{x}_{i-\frac{1}{2}}}u_h^+(x_{i-\frac{1}{2}}). \tag{3.23}$$

For simplicity, we denote $t^{i+\frac{1}{2}}(x) := s^{i+\frac{1}{2}}\left(\xi^{i+\frac{1}{2}}(x)\right)_x$. By using the chain rule, we know that

$$t^{i+\frac{1}{2}}(x) = s_\xi^{i+\frac{1}{2}}\xi_x^{i+\frac{1}{2}} = \frac{2}{\triangle\tilde{x}_{i+\frac{1}{2}}}\left(3\xi_{i+\frac{1}{2}} + 15(3\xi_{i+\frac{1}{2}}^2 - 1)\frac{x - \tilde{x}_{i+\frac{1}{2}}}{\triangle\tilde{x}_{i+\frac{1}{2}}}\right).$$

Notice that $t^{i+\frac{1}{2}}(x)$ is linear in x, and it is easy to get

$$\max_{x\in[\tilde{x}_i, x_{i+\frac{1}{2}}]} t^{i+\frac{1}{2}}(x) = \frac{6}{\triangle\tilde{x}_{i+\frac{1}{2}}}h(\xi_{i+\frac{1}{2}}), \qquad \max_{x\in[x_{i-\frac{1}{2}}, \tilde{x}_i]}\{-t^{i-\frac{1}{2}}(x)\} = \frac{6}{\triangle\tilde{x}_{i-\frac{1}{2}}}h(-\xi_{i+\frac{1}{2}}),$$

Also, it is obvious that

$$h(\xi) \le h(|\xi|), \qquad \xi \in [-1, 1].$$

Hence, the upper bound for the integration terms in (3.23) can be estimated as

$$\begin{aligned}
&\frac{1}{\triangle x_i \triangle \tilde{x}_{i+\frac{1}{2}}} \int_{\tilde{x}_i}^{x_{i+\frac{1}{2}}} u_h t^{i+\frac{1}{2}}(x) dx - \frac{1}{\triangle x_i \triangle \tilde{x}_{i-\frac{1}{2}}} \int_{x_{i-\frac{1}{2}}}^{\tilde{x}_i} u_h t^{i-\frac{1}{2}}(x) dx \\
\le &\frac{\int_{\tilde{x}_i}^{x_{i+\frac{1}{2}}} u_h \, dx}{\triangle x_i} \max_{x \in [\tilde{x}_i, x_{i+\frac{1}{2}}]} \frac{t^{i+\frac{1}{2}}(x)}{\triangle \tilde{x}_{i+\frac{1}{2}}} + \frac{\int_{x_{i-\frac{1}{2}}}^{\tilde{x}_i} u_h \, dx}{\triangle x_i} \max_{x \in [x_{i-\frac{1}{2}}, \tilde{x}_i]} \frac{-t^{i-\frac{1}{2}}(x)}{\triangle \tilde{x}_{i-\frac{1}{2}}} \le \frac{6\bar{u}_i^n}{\triangle x^2} \max_i h(|\xi_{i+\frac{1}{2}}|).
\end{aligned} \tag{3.24}$$

For the other terms in (3.23), we can use the same idea for solving $p_h(x_{i+\frac{1}{2}})$ in (3.9) and map $x \in I_i$ onto the standard element $\eta \in [-1, 1]$. Then we can compute the point value of u_h as an integration

$$u_h(x(\eta_0)) := u_0(\eta_0) = \frac{1}{2} \int_{-1}^{1} u_0(\eta) r(\eta_0, \eta) d\eta, \quad \forall \eta_0 \in [-1, 1],$$

where

$$r(\eta_0, \eta) = 1 + 3\eta_0 \eta + \frac{5}{4}(3\eta_0^2 - 1)(3\eta^2 - 1).$$

Hence, the rest terms in (3.23) become

$$\begin{aligned}
&\left(\frac{s^{i+\frac{1}{2}}(-1)}{\triangle x_i \triangle \tilde{x}_{i+\frac{1}{2}}} + \frac{s^{i-\frac{1}{2}}(1)}{\triangle x_i \triangle \tilde{x}_{i-\frac{1}{2}}} \right) u_h(\tilde{x}_i) + \frac{\alpha_{i+\frac{1}{2}}}{\triangle x_i \triangle \tilde{x}_{i+\frac{1}{2}}} u_h^-(x_{i+\frac{1}{2}}) + \frac{\alpha_{i-\frac{1}{2}}}{\triangle x_i \triangle \tilde{x}_{i-\frac{1}{2}}} u_h^+(x_{i-\frac{1}{2}}) \\
= &\frac{1}{2\triangle x_i} \int_{-1}^{1} u_0(\eta) R(\eta) d\eta \le \frac{\bar{u}_i^n}{\triangle x_i} \max_{\eta \in [-1,1]} R(\eta),
\end{aligned} \tag{3.25}$$

where

$$R(\eta) = \left[\frac{s^{i+\frac{1}{2}}(-1)}{\triangle \tilde{x}_{i+\frac{1}{2}}} + \frac{s^{i-\frac{1}{2}}(1)}{\triangle \tilde{x}_{i-\frac{1}{2}}} \right] r(\xi_0, \eta) + \frac{\alpha_{i+\frac{1}{2}}}{\triangle \tilde{x}_{i+\frac{1}{2}}} r(1, \eta) + \frac{\alpha_{i-\frac{1}{2}}}{\triangle \tilde{x}_{i-\frac{1}{2}}} r(-1, \eta),$$

and we have used $u_0(\eta) \ge 0$ for $\eta \in [-1, 1]$ in the last step. By simple computations, we know that

$$\max_{\eta \in [-1,1]} |r(\eta_0, \eta)| \le \ell(\eta_0) \le 9, \qquad \eta_0 \in [-1, 1].$$

Since $s^{i+\frac{1}{2}}(\xi) = r(\xi_{i+\frac{1}{2}}, \xi)$, we have

$$\begin{aligned}
R(\eta) &\le \left[\frac{|r(\xi_{i+\frac{1}{2}}, -1)|}{\triangle \tilde{x}_{i+\frac{1}{2}}} + \frac{|r(\xi_{i-\frac{1}{2}}, 1)|}{\triangle \tilde{x}_{i-\frac{1}{2}}} \right] |r(\xi_0, \eta)| + \frac{\alpha_{i+\frac{1}{2}}}{\triangle \tilde{x}_{i+\frac{1}{2}}} |r(1, \eta)| + \frac{\alpha_{i-\frac{1}{2}}}{\triangle \tilde{x}_{i-\frac{1}{2}}} |r(-1, \eta)| \\
&\le \frac{18}{\triangle x} \ell(\xi_0) + \frac{18}{\triangle x} \max_i \alpha_{i+\frac{1}{2}}.
\end{aligned} \tag{3.26}$$

Combing Eqs. (3.23), (3.24), (3.25), and (3.26), we have

$$-\frac{U_i}{\triangle x_i} \le \frac{6\bar{u}_i^n}{\triangle x^2} \left[\max_i h(|\xi_{i+\frac{1}{2}}|) + 3\ell(\xi_0) + 3 \max_i \alpha_{i+\frac{1}{2}} \right], \tag{3.27}$$

and thus can obtain the conclusion. □

Remark 3.1. Notice that we have only given a very rough estimate of the upper bound of $-\frac{U_i}{\triangle x_i}$ in (3.27) to show that $\bar{u}_i^n + \frac{\triangle t}{\triangle x_i} U_i$ can be non-negative with a small $\triangle t$. In practice, the real upper bound of $-\frac{U_i}{\triangle x_i}$ may be much smaller and hence $\triangle t$ can be much larger than the one in (3.20).

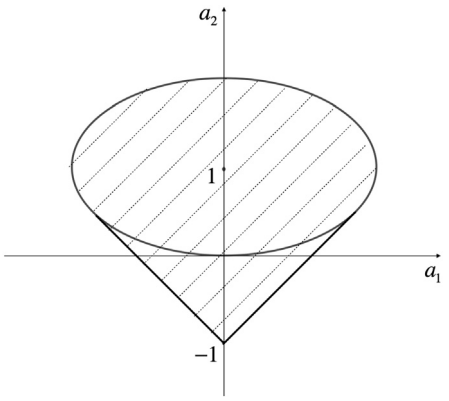

Fig. 3.1. Corresponding region in a_1a_2 plane when $u_1(\eta) \geq 0$ for $\eta \in [-1, 1]$.

Now, we proceed to analyze U_{i+1} and U_{i-1}. In this step, we need to find the requirement on $\alpha_{i+\frac{1}{2}}$ to make $U_{i+1} \geq 0$. We assume that $u_h(x) \geq 0$ in $I_{i+1} = [x_{i+\frac{1}{2}}, x_{i+\frac{3}{2}}]$. For simplicity, we map $x \in I_{i+1}$ onto the standard element $[-1, 1]$:

$$x = x_{i+1} + \frac{\triangle x_{i+1}}{2}\eta, \qquad \eta \in [-1, 1],$$

and consider u_h as a function of η on the standard element:

$$u_h(x(\eta)) = u_1(\eta) = a_0 + a_1L_1(\eta) + a_2L_2(\eta), \quad \eta \in [-1, 1].$$

Notice that U_{i+1} is linear with respect to u_h and

$$a_0 = \frac{1}{2}\int_{-1}^{1} u_1(x(\eta))d\eta \geq 0.$$

We only need to consider the case with

$$u_1(\eta) = 1 + a_1L_1(\eta) + a_2L_2(\eta),\ \eta \in [-1, 1].$$

We first illustrate a lemma to show the equivalent requirement on a_1 and a_2 when $u_1 \geq 0$.

Lemma 3.3. *$u_1(\eta) = 1 + a_1L_1(\eta) + a_2L_2(\eta) \geq 0$ for any $\eta \in [-1, 1]$ if and only if*

$$\begin{cases} 1 \pm a_1 + a_2 \geq 0, & \text{when } |a_1| \geq 3a_2, \\ \frac{a_1^2}{3} + (a_2 - 1)^2 \leq 1, & \text{when } |a_1| < 3a_2. \end{cases}$$

Proof. If the parabola $u_1(\eta)$ opens downward, i.e. $a_2 < 0$, then $u_1(\eta) \geq 0$ in $[-1, 1]$ if and only if

$$u_1(-1) = 1 - a_1 + a_2 \geq 0 \qquad \text{and} \qquad u_1(1) = 1 + a_1 + a_2 \geq 0. \tag{3.28}$$

If $a_2 = 0$ and hence $u_1(\eta)$ is a linear polynomial, then we also have $u_1(\eta) \geq 0$ in $[-1, 1]$ if and only if (3.28) is satisfied. If the parabola $u_1(\eta)$ opens upward and the symmetry axis $-\frac{a_1}{3a_2}$ lies out of $[-1, 1]$, i.e. $a_2 > 0$ and $\frac{|a_1|}{3a_2} \geq 1$, then $u_1(\eta) \geq 0$ in $[-1, 1]$ if and only if (3.28) is satisfied. Finally, if the parabola $u_1(\eta)$ opens upward and the symmetry axis lies within $[-1, 1]$, i.e. $a_2 > 0$ and $\frac{|a_1|}{3a_2} < 1$, then $u_1 \geq 0$ if and only if $\min u_1 = 1 - \frac{3a_2^2 + a_1^2}{6a_2} \geq 0$, that is

$$\frac{a_1^2}{3} + (a_2 - 1)^2 \leq 1.$$

Combing all the cases above, we get the conclusion. □

We can easily see that (a_1, a_2) falls into the shaded region in Fig. 3.1 when the requirements in the above lemma are satisfied. It is easy to verify that the line $1 \pm a_1 + a_2 = 0$ is tangent to the ellipse $\frac{a_1^2}{3} + (a_2 - 1)^2 = 1$ at the point $(\mp\frac{3}{2}, \frac{1}{2})$ and hence the region in Fig. 3.1 is convex. Since U_{i+1} is linear with respect to u_h, we only need to consider the following two special cases.

1. **Case 1:** $a_1 = 0$ and $a_2 = -1$.
In this case, we can get

$$U_{i+1} = \frac{3(\xi_0+1)}{16}\left[45\xi_{i+\frac{1}{2}}^4 + 30\xi_{i+\frac{1}{2}}^3 - 14\xi_{i+\frac{1}{2}} - 2\xi_{i+\frac{1}{2}} + 13 - 3(\xi_{i+\frac{1}{2}}+1)^2(5\xi_{i+\frac{1}{2}}^2+1)\xi_0\right].$$

To make $U_{i+1} \geq 0$, we need

$$\xi_0 \leq \min_{\xi_{i+\frac{1}{2}}\in[-1,1]} \frac{45\xi_{i+\frac{1}{2}}^4 + 30\xi_{i+\frac{1}{2}}^3 - 14\xi_{i+\frac{1}{2}}^2 - 2\xi_{i+\frac{1}{2}} + 13}{3(\xi_{i+\frac{1}{2}}+1)^2(5\xi_{i+\frac{1}{2}}^2+1)} = \frac{29}{9} - \frac{26\sqrt{6}}{27} \approx 0.8635. \tag{3.29}$$

Notice that $\xi_{i+\frac{1}{2}}$ is a function of ξ_0 and $\frac{\triangle x_i}{\triangle x_{i+1}}$ as shown in (3.6), we would like to adjust ξ_0 such that $U_{i+1} \geq 0$ for any $\xi_{i+\frac{1}{2}} \in [-1, 1]$. That is, we do not restrict the mesh sizes ratio $\frac{\triangle x_i}{\triangle x_{i+1}}$.

2. **Case 2:** the boundary of the ellipse, i.e., $\frac{a_1^2}{3} + (a_2-1)^2 = 1$.
In this case, we have

$$U_{i+1} = \frac{\xi_0+1}{4}\left(\Gamma + b_1a_1 + b_2a_2\right),$$

where

$$\Gamma = \frac{4}{\xi_0+1}\left[\alpha_{i+\frac{1}{2}} + 1 + 3\xi_{i+\frac{1}{2}}^2 + \frac{5}{4}(3\xi_{i+\frac{1}{2}}^2 - 1)^2\right],$$
$$b_1 = \xi_{i+\frac{1}{2}}(\xi_{i+\frac{1}{2}}+1)(15\xi_{i+\frac{1}{2}}^2+1) + 4 - \Gamma,$$
$$b_2 = \Gamma - \frac{3}{4}\left(45\xi_{i+\frac{1}{2}}^4 + 30\xi_{i+\frac{1}{2}}^3 - 14\xi_{i+\frac{1}{2}}^2 - 2\xi_{i+\frac{1}{2}} + 13\right) + \frac{9\xi_0}{4}(\xi_{i+\frac{1}{2}}+1)^2(5\xi_{i+\frac{1}{2}}^2+1).$$

To make $U_{i+1} \geq 0$, we need

$$\Gamma + b_1a_1 + b_2a_2 = \Gamma + b_2 + b_1a_1 + b_2(a_2-1) \geq 0,$$

i.e.

$$\Gamma + b_2 \geq -[b_1a_1 + b_2(a_2-1)].$$

Since $\frac{a_1^2}{3} + (a_2-1)^2 = 1$, we need to have

$$\Gamma + b_2 \geq \sqrt{3b_1^2 + b_2^2},$$

which is equivalent to the following requirement on the penalty coefficient

$$\begin{aligned}\alpha_{i+\frac{1}{2}} &\geq \frac{[\xi_{i+\frac{1}{2}}(\xi_{i+\frac{1}{2}}+1)(15\xi_{i+\frac{1}{2}}^2+1)+4]^2}{6(5\xi_{i+\frac{1}{2}}^2+1)(\xi_{i+\frac{1}{2}}+1)^2} - \frac{5}{4}(3\xi_{i+\frac{1}{2}}^2-1)^2 - 3\xi_{i+\frac{1}{2}}^2 - 1 \\ &:= g(dx_{i+\frac{1}{2}}, \xi_0),\end{aligned} \tag{3.30}$$

where we have used (3.6) and represent $\xi_{i+\frac{1}{2}}$ as a function of ξ_0 and $dx_{i+\frac{1}{2}}$. The analysis above can be summarized as the following lemma.

Lemma 3.4. *Suppose $u_h \geq 0$ in I_{i+1} and the conditions in (3.29) and (3.30) are satisfied, then $U_{i+1} \geq 0$. Similarly, if $u_h \geq 0$ in I_{i-1} and*

$$\xi_0 \geq \frac{26\sqrt{6}}{27} - \frac{29}{9} \qquad \text{and} \qquad \alpha_{i-\frac{1}{2}} \geq g(1/dx_{i-\frac{1}{2}}, -\xi_0), \tag{3.31}$$

then we have $U_{i-1} \geq 0$.

Based on the above lemma, we should choose $\xi_0 \in [\frac{26\sqrt{6}}{27} - \frac{29}{9}, \frac{29}{9} - \frac{26\sqrt{6}}{27}]$. Also, $\alpha_{i+\frac{1}{2}}$ at a fixed boundary $x_{i+\frac{1}{2}}$ should satisfy

$$\alpha_{i+\frac{1}{2}} \geq \max\{g(dx_{i+\frac{1}{2}}, \xi_0),\ g(1/dx_{i+\frac{1}{2}}, -\xi_0)\} := \tilde{g}(dx_{i+\frac{1}{2}}, \xi_0). \tag{3.32}$$

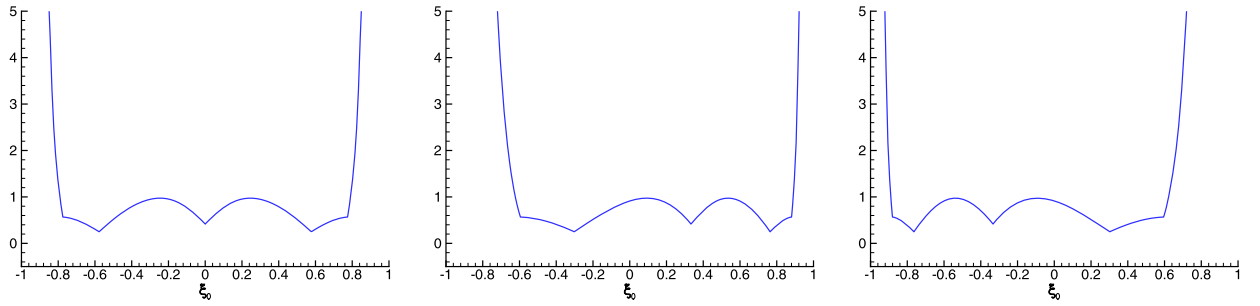

(a) $dx_{i+\frac{1}{2}} = 1$ (b) $dx_{i+\frac{1}{2}} = 2$ (c) $dx_{i+\frac{1}{2}} = 1/2$

Fig. 3.2. Plots of $\tilde{g}(dx_{i+\frac{1}{2}}, \xi_0)$ for different given $dx_{i+\frac{1}{2}}$.

Recall that $dx_{i+\frac{1}{2}} = \frac{\triangle x_i}{\triangle x_{i+1}}$. In practice when the computational mesh is given, which can be non-uniform, $dx_{i+\frac{1}{2}}$ can be computed for each fixed i. Next, we just fix the value of $dx_{i+\frac{1}{2}}$ for a fixed i and try to adjust ξ_0 such that $\alpha_{i+\frac{1}{2}}$ can be minimized. By simple computations, we have

$$\min_{\xi_0} \tilde{g}(dx_{i+\frac{1}{2}}, \xi_0) = 1/4,$$

and there are two critical points

$$\xi_0^1 = \frac{dx_{i+\frac{1}{2}}^2 - 2\sqrt{3}dx_{i+\frac{1}{2}} - 1}{dx_{i+\frac{1}{2}}^2 + 4dx_{i+\frac{1}{2}} + 1}, \quad \xi_0^2 = \frac{dx_{i+\frac{1}{2}}^2 + 2\sqrt{3}dx_{i+\frac{1}{2}} - 1}{dx_{i+\frac{1}{2}}^2 + 4dx_{i+\frac{1}{2}} + 1}.$$

Fig. 3.2 shows the plots of $\tilde{g}(dx_{i+\frac{1}{2}}, \xi_0)$ with respect to $\xi_0 \in [-1, 1]$ for different given $dx_{i+\frac{1}{2}}$. If $dx_{i+\frac{1}{2}} = 1$, then the mesh is uniform and ξ_0^1 and ξ_0^2 are the roots of the Legendre polynomial of degree two,

$$\xi_0^1 = -\frac{\sqrt{3}}{3}, \qquad \xi_0^2 = \frac{\sqrt{3}}{3}.$$

Also, for $\xi_0 = 0$, i.e. the dual mesh is generated by the midpoint of the primitive mesh, we have

$$\tilde{g}(1, 0) = 5/12.$$

When $dx_{i+\frac{1}{2}} = 2$, we can take

$$\xi_0^1 = -\frac{4\sqrt{3} - 3}{13}, \qquad \xi_0^2 = \frac{4\sqrt{3} + 3}{13}.$$

When $dx_{i+\frac{1}{2}} = 1/2$, we can take

$$\xi_0^1 = -\frac{4\sqrt{3} + 3}{13}, \qquad \xi_0^2 = \frac{4\sqrt{3} - 3}{13}.$$

Finally, we would like to point out that for fixed $dx_{i+\frac{1}{2}}$, $\tilde{g} \to \infty$ as $|\xi_0| \to 1$. Therefore, we cannot construct third-order MPP technique for the original LDG method, and our conclusion does not violate that given in [30].

Step 4: PP technique for nonlinear case

In this step, we will discuss the PP technique for nonlinear problems. We assume $u_h \geq 0$ which further implies $A(u_h) \geq 0$. To apply the same analysis for the linear case, we would like to replace $A(u_h)$ in (2.3) by a piecewise quadratic polynomial $\tilde{A}(x) \geq 0$ such that $\tilde{A}(x)|_{I_i} \in P^2(I_i)$ and for any $i = 1, \cdots, N_x$

$$\tilde{A}_{i+\frac{1}{2}}^- = A\left((u_h)_{i+\frac{1}{2}}^-\right), \quad \tilde{A}_{i-\frac{1}{2}}^+ = A\left((u_h)_{i-\frac{1}{2}}^+\right), \quad \|\tilde{A}\|_{L^\infty(I_i)} \leq \tilde{C}\|A(u_h)\|_{L^\infty(I_i)}. \tag{3.33}$$

Then U_i, U_{i+1} and U_{i-1} in (3.14), (3.15) and (3.16) can be written as

$$U_i = \frac{\hat{a}_{i+\frac{1}{2}}}{\triangle\tilde{x}_{i+\frac{1}{2}}}\left[-\int_{\tilde{x}_i}^{x_{i+\frac{1}{2}}} \tilde{A}s^{i+\frac{1}{2}}\left(\xi^{i+\frac{1}{2}}(x)\right)_x dx - A(\tilde{x}_i)s^{i+\frac{1}{2}}(-1) - \alpha_{i+\frac{1}{2}}\tilde{A}^-_{i+\frac{1}{2}}\right]$$
$$- \frac{\hat{a}_{i-\frac{1}{2}}}{\triangle\tilde{x}_{i-\frac{1}{2}}}\left[-\int_{x_{i-\frac{1}{2}}}^{\tilde{x}_i} \tilde{A}s^{i-\frac{1}{2}}\left(\xi^{i-\frac{1}{2}}(x)\right)_x dx + A(\tilde{x}_i)s^{i-\frac{1}{2}}(1) + \alpha_{i-\frac{1}{2}}A^+_{i-\frac{1}{2}}\right], \tag{3.34}$$

$$U_{i+1} = \int_{x_{i+\frac{1}{2}}}^{\tilde{x}_{i+1}} \tilde{A}_x s^{i+\frac{1}{2}}\left(\xi^{i+\frac{1}{2}}(x)\right)dx + A^+_{i+\frac{1}{2}}\left[s^{i+\frac{1}{2}}(\xi_{i+\frac{1}{2}}) + \alpha_{i+\frac{1}{2}}\right], \tag{3.35}$$

$$U_{i-1} = -\int_{\tilde{x}_{i-1}}^{x_{i-\frac{1}{2}}} \tilde{A}_x s^{i-\frac{1}{2}}\left(\xi^{i-\frac{1}{2}}(x)\right)dx + A^-_{i-\frac{1}{2}}\left[s^{i-\frac{1}{2}}(\xi_{i-\frac{1}{2}}) + \alpha_{i-\frac{1}{2}}\right]. \tag{3.36}$$

The construction of $\tilde{A}$ will be discussed in the "Implementation". Now, we can demonstrate the positivity of D_i in (3.13). Following the same proof of Lemma 3.4 we have

Lemma 3.5. *Suppose U_{i+1} and U_{i-1} are given in (3.35) and (3.36), respectively, then $U_{i+1} \geq 0$ and $U_{i-1} \geq 0$ under the conditions*

$$\frac{26\sqrt{6}}{27} - \frac{29}{9} \leq \xi_0 \leq \frac{29}{9} - \frac{26\sqrt{6}}{27} \quad \text{and} \quad \alpha_{i-\frac{1}{2}} \geq \max\left\{g(1/dx_{i-\frac{1}{2}}, -\xi_0), g(dx_{i-\frac{1}{2}}, \xi_0)\right\}, \tag{3.37}$$

where g is defined in (3.30).

The estimate of U_i given in (3.34) can be obtained below.

Lemma 3.6. *Suppose $u_h \geq 0$ in I_i, then $\bar{u}_h + \frac{2\Delta t}{\Delta x_i}U_i \geq 0$ under the condition*

$$\triangle t \leq \frac{\mu_2 \triangle x^2}{12\mu_1\tilde{C}\max_u a^2(u)\left[\max_i h(|\xi_{i+\frac{1}{2}}|) + 3\ell(\xi_0) + 3\max_i \alpha_{i+\frac{1}{2}}\right]}, \tag{3.38}$$

where h and ℓ were defined in (3.21) and (3.22), respectively, and μ_1 and μ_2 are the parameters used in the following norm equivalence for P^2 polynomials:

$$\mu_1\|u_h\|_{L^\infty(I_i)} \geq \bar{u}_i^n \geq \mu_2\|u_h\|_{L^\infty(I_i)}. \tag{3.39}$$

Proof. Following the same analysis for (3.27), we have

$$-\frac{\tilde{U}_i}{\triangle x_i} \leq \frac{6\bar{u}_i^n \max_u a(u)}{\triangle x^2}\left[\max_i h(|\xi_{i+\frac{1}{2}}|) + 3\ell(\xi_0) + 3\max_i \alpha_{i+\frac{1}{2}}\right].$$

Therefore, we have

$$\overline{\tilde{A}} + \frac{\Delta t}{\Delta x_i \max_u a(u)}\tilde{U}_i \geq 0$$

under the condition (3.20). Now, we find the relationship between $\overline{\tilde{A}}$ and $\bar{u}_h$:

$$\overline{\tilde{A}} \leq \mu_1\|\tilde{A}\|_{L^\infty(I_i)} \leq \mu_1\tilde{C}\|A(u_h)\|_{L^\infty(I_i)} \leq \mu_1\tilde{C}\max_u a(u)\|u_h\|_{L^\infty(I_i)} \leq \frac{\mu_1\tilde{C}}{\mu_2}\max_u a(u)\bar{u}_h,$$

where in the first and last steps, we applied the norm equivalence, step two requires Lemma 3.7 and the third step is the mean value theorem. □

Remark 3.2. (3.39) follows from the norm equivalence. Notice that we assume the numerical approximation $u_h \geq 0$ in cell I_i, then

$$\bar{u}_i = \frac{1}{\Delta x_i}\int_{I_i} u_h dx = \frac{1}{\Delta x_i}\|u_h\|_{L^1(I_i)}.$$

Since u_h is a polynomial of degree 2, by the norm equivalence in finite dimension spaces and the scaling argument, we can find two constants μ_1 and μ_2 such that

$$\mu_1\|u_h\|_{L^\infty(I_i)} \geq \frac{1}{\Delta x_i}\|u_h\|_{L^1(I_i)} \geq \mu_2\|u_h\|_{L^\infty(I_i)},$$

which further yields (3.39).

The above two lemmas yield a straightforward corollary.

Corollary 3.1. *Suppose the conditions in the above two lemmas are satisfied, if $u_h^n \geq 0$, then $\bar{u}^{n+1} \geq 0$. Moreover, if $u_h^n \leq 0$, then $\bar{u}^{n+1} \leq 0$.*

Remark 3.3. In (3.38), the time step will be very small. If we enforce the time step, the computational cost for time is actually very high. Moreover, it will be extremely difficult to construct the PP limiter with implicit Euler method, and we will discuss this in the future.

Step 5: MPP technique for the nonlinear case

Now we can proceed to the MPP technique. We also need to replace $A(u_h)$ in (2.3) with a piecewise quadratic polynomial $\tilde{A}(x)$ such that (3.33) is satisfied and

$$\int_0^m a(u)\,du \leq \tilde{A}(x) \leq \int_0^M a(u)\,du,$$

and the result is given in the following theorem.

Theorem 3.1. *Suppose $m \leq u_h \leq M$, and the conditions in Lemmas 3.5 and 3.6 are satisfied, then we have $m \leq \bar{u}_i^{n+1} \leq M$.*

Proof. We only prove $m \leq \bar{u}_i^{n+1}$, since the other inequality can be obtained following the same lines with minor changes. Define $v_h = u_h - m$, then $v_h \geq 0$ and define

$$B(v_h) = A(u_h) = \int_0^{u_h} a(u)\,du = \int_{-m}^{v_h} a(v+m)\,dv. \tag{3.40}$$

Therefore, D_i in (3.13) can be written as

$$D_i - m = \bar{v}_i^n + \frac{2\triangle t}{\triangle x_i}V_i + \frac{2\triangle t\hat{a}_{i+\frac{1}{2}}}{\triangle x_i\triangle\tilde{x}_{i+\frac{1}{2}}}V_{i+1} + \frac{2\triangle t\hat{a}_{i-\frac{1}{2}}}{\triangle x_i\triangle\tilde{x}_{i-\frac{1}{2}}}V_{i-1},$$

where

$$V_i = \frac{\hat{a}_{i+\frac{1}{2}}}{\triangle\tilde{x}_{i+\frac{1}{2}}}\left[-\int_{\tilde{x}_i}^{x_{i+\frac{1}{2}}} B(v_h)s^{i+\frac{1}{2}}\left(\xi^{i+\frac{1}{2}}(x)\right)_x dx - B(v_h(\tilde{x}_i))s^{i+\frac{1}{2}}(-1) - \alpha_{i+\frac{1}{2}}B(v_h^-(x_{i+\frac{1}{2}}))\right]$$
$$- \frac{\hat{a}_{i-\frac{1}{2}}}{\triangle\tilde{x}_{i-\frac{1}{2}}}\left[-\int_{x_{i-\frac{1}{2}}}^{\tilde{x}_i} B(v_h)s^{i-\frac{1}{2}}\left(\xi^{i-\frac{1}{2}}(x)\right)_x dx + B(v_h(\tilde{x}_i))s^{i-\frac{1}{2}}(1) + \alpha_{i-\frac{1}{2}}B(v_h^+(x_{i-\frac{1}{2}}))\right],$$

$$V_{i+1} = \int_{x_{i+\frac{1}{2}}}^{\tilde{x}_{i+1}} B(v_h)_x s^{i+\frac{1}{2}}\left(\xi^{i+\frac{1}{2}}(x)\right) dx + B(v_h^+(x_{i+\frac{1}{2}}))\left[s^{i+\frac{1}{2}}(\xi_{i+\frac{1}{2}}) + \alpha_{i+\frac{1}{2}}\right],$$

$$V_{i-1} = -\int_{\tilde{x}_{i-1}}^{x_{i-\frac{1}{2}}} B(v_h)_x s^{i-\frac{1}{2}}\left(\xi^{i-\frac{1}{2}}(x)\right) dx + B(v_h^-(x_{i-\frac{1}{2}}))\left[s^{i-\frac{1}{2}}(\xi_{i-\frac{1}{2}}) + \alpha_{i-\frac{1}{2}}\right].$$

It is easy to check that in the definition of B in (3.40), we can replace the lower limiter in the integral by any constants without changing the value of D_i. Therefore, we may assume $B(v_h) = \int_0^{v_h} a(v+m)\, dv$. Now, following (3.33), we can replace B by $\tilde{B}$ to compute D_i. Then the analyses in previous steps can be applied directly to obtain $D_i - m \geq 0$, which further yield $D_i \geq m$. By Lemma 3.1, we have $m \leq \bar{u}_i^{n+1}$. □

3.2. Implementation

In this subsection, we will demonstrate how to implement the MPP LDG method. WLOG, we assume $A(u_h) = \int_0^{u_h} a(u)\, du$ and $m \leq u_h \leq M$. We further denote $\tilde{m} = \int_0^m a(u)\, du$ and $\tilde{M} = \int_0^M a(u)\, du$, and hence $\tilde{m} \leq A(u_h) \leq \tilde{M}$. We use the following steps to construct a quadratic polynomial $\tilde{A}$ in each element I_i such that $\tilde{m} \leq \tilde{A} \leq \tilde{M}$:

1. Compute a linear function $p_1 \in P^1(I_i)$ such that p_1 is the interpolation of $A(u_h)$ at $x = x_{i-\frac{1}{2}}$ and $x = x_{i+\frac{1}{2}}$. Since $\tilde{m} \leq A(u_h) \leq \tilde{M}$, it is obvious that $p_1(x) \in [\tilde{m}, \tilde{M}]$, $\forall x \in I_i$.
2. Calculate a quadratic polynomial $p_2 \in P^2(I_i)$ such that p_2 is the interpolation of $A(u_h)$ at $x = x_{i-\frac{1}{2}}$, $x = x_i$ and $x = x_{i+\frac{1}{2}}$. It is possible that $\min_{x\in I_i} p_2(x) < \tilde{m}$ or $\max_{x\in I_i} p_2(x) > \tilde{M}$, but they will not happen simultaneously.
3. Combine p_1 and p_2 to get $\tilde{A} = \theta p_2 + (1-\theta)p_1$, where $\theta \in [0,1]$ is the largest possible value such that $\tilde{m} \leq \tilde{A} \leq \tilde{M}$. This can always be done since in the extreme case when $\theta = 0$ we have $\tilde{A} = p_1 \in [\tilde{m}, \tilde{M}]$.

Remark. In the case that $\min_{x\in I_i} p_2(x) < \tilde{m}$, we can solve $\min_{x\in I_i}[\theta p_2(x) + (1-\theta)p_1(x)] = \tilde{m}$ to get θ. If there are multiple solutions, we just take the largest one within the region [0,1]. In the case that $\max_{x\in I_i} p_2(x) > \tilde{M}$, we can simply solve $\max_{x\in I_i}[\theta p_2(x) + (1-\theta)p_1(x)] = \tilde{M}$ to get θ.

Lemma 3.7. *Suppose $\tilde{A}$ is constructed above, then there exists a positive constant C such that*

$$\|\tilde{A}\|_{L^\infty(I_i)} \leq C\|A(u_h)\|_{L^\infty(I_i)}.$$

Proof. It is easy to see that

$$\|p_2\|_{L^\infty(I_i)} \leq C\|A(u_h)\|_{L^\infty(I_i)}, \quad \|p_1\|_{L^\infty(I_i)} \leq \|A(u_h)\|_{L^\infty(I_i)}.$$

Finally, the conclusion follows from triangle inequality directly. □

With Theorem 3.1, the numerical cell average $\bar{u}_i^{n+1} \in [m, M]$. However, the numerical approximation u_h^{n+1} may be out of the bounds. Therefore, we also need to apply some limiter to u_h^{n+1} and the procedure is given below. For simplicity, we will drop the superscript $n+1$.

1. Set up a small number $\epsilon = 10^{-13}$.
2. If $\bar{u}_h \leq m + \epsilon$ or $\bar{u}_h \geq M - \epsilon$, take $u_h = \bar{u}_h$. Then skip the following steps.
3. Define $m_i = \min_{x\in I_i} u_h(x)$ and $M_i = \max_{x\in I_i} u_h(x)$. Set $\theta = 1$. If $m_i < m$ or $M_i > M$, then take
$$\theta = \max\left\{\frac{\bar{u}_h - m - \epsilon}{\bar{u}_h - m_i}, \frac{\bar{u}_h - M + \epsilon}{\bar{u}_h - M_i}\right\}.$$
4. Apply the slope limiter $\tilde{u}_h = \bar{u}_h + \theta(u_h - \bar{u}_h)$, and use $\tilde{u}_h$ as the new numerical approximation.

Remark. We still use the notation θ here but it is not the same one used to compute $\tilde{A}$. Similar rule applies to the two dimensional problem to be discussed in Section 4.

In [27], the authors have proved that the limiter keeps the high-order accuracy.

3.3. High-order time integrations

All the previous analyses are based on first-order Euler forward time discretization. We can also use strong stability preserving (SSP) high-order time discretizations to solve the ODE system $\mathbf{w}_t = \mathbf{L}\mathbf{w}$. More details of these time discretizations can be found in [24,23,13]. In this paper, we use the third-order SSP Runge–Kutta method [24]

$$\begin{aligned}
\mathbf{w}^{(1)} &= \mathbf{w}^n + \Delta t \mathbf{L}(\mathbf{w}^n), \\
\mathbf{w}^{(2)} &= \frac{3}{4}\mathbf{w}^n + \frac{1}{4}\left(\mathbf{w}^{(1)} + \Delta t \mathbf{L}(\mathbf{w}^{(1)})\right), \\
\mathbf{w}^{n+1} &= \frac{1}{3}\mathbf{w}^n + \frac{2}{3}\left(\mathbf{w}^{(2)} + \Delta t \mathbf{L}(\mathbf{w}^{(2)})\right),
\end{aligned} \tag{3.41}$$

and the third order SSP multi-step method [23]

$$\mathbf{w}^{n+1} = \frac{16}{27}\left(\mathbf{w}^n + 3\Delta t \mathbf{L}(\mathbf{w}^n)\right) + \frac{11}{27}\left(\mathbf{w}^{n-3} + \frac{12}{11}\Delta t \mathbf{L}(\mathbf{w}^{n-3})\right). \tag{3.42}$$

4. LDG scheme on overlapping meshes in two space dimensions

In this section, we will construct the third-order MPP LDG scheme on overlapping meshes in two space dimensions and, for simplicity, we study the following pure diffusion equation over the domain $\Omega = [0,1]\times[0,1]$,

$$\begin{cases} u_t = (a(u)p)_x + (b(u)q)_y, \\ p = A(u)_x, \\ q = B(u)_y, \end{cases} \tag{4.1}$$

subject to periodic boundary conditions, where $A(u) = \int^u a(t)dt$ and $B(u) = \int^u b(t)dt$.

We first define the primitive mesh for the primary variable u which is a regular rectangular decomposition of Ω. Let $0 = x_{\frac{1}{2}} < x_{\frac{3}{2}} < \cdots < x_{N_x+\frac{1}{2}} = 1$ and $0 = y_{\frac{1}{2}} < y_{\frac{3}{2}} < \cdots < y_{N_y+\frac{1}{2}} = 1$ be grid points in x and y directions, respectively. We denote the i,j-th cell as

$$I_{ij} = I_i \times J_j, \quad i = 1,\cdots,N_x,\ j = 1,\cdots,N_y,$$

where $I_i = [x_{i-\frac{1}{2}}, x_{i+\frac{1}{2}}]$ and $J_j = [y_{j-\frac{1}{2}}, y_{j+\frac{1}{2}}]$. Moreover, we denote

$$\Delta x_i = x_{i+\frac{1}{2}} - x_{i-\frac{1}{2}}, \quad x_i = \frac{x_{i-\frac{1}{2}} + x_{i+\frac{1}{2}}}{2}, \quad \Delta y_j = y_{j+\frac{1}{2}} - y_{j-\frac{1}{2}}, \quad y_j = \frac{y_{j-\frac{1}{2}} + y_{j+\frac{1}{2}}}{2}.$$

Moreover, we define $\Delta x = \min_i \Delta x_i$ and $\Delta y = \min_j \Delta y_j$. We also move each cell horizontally to obtain the P-mesh: $P_{i+\frac{1}{2},j} = P_{i+\frac{1}{2}} \times J_j$, where

$$P_{i+\frac{1}{2}} = [\tilde{x}_i, \tilde{x}_{i+1}], \qquad \tilde{x}_i = x_i + \frac{\Delta x_i}{2}\xi_0, \qquad \xi_0 \in [-1,1], \qquad i = 1,2,\cdots,N_x, \tag{4.2}$$

with $\tilde{x}_0 = \tilde{x}_{N_x} - 1$. Similarly, we can define the Q-mesh: $Q_{i,j+\frac{1}{2}} = I_i \times Q_{j+\frac{1}{2}}$, where

$$Q_{j+\frac{1}{2}} = [\tilde{y}_j, \tilde{y}_{j+1}], \qquad \tilde{y}_j = y_j + \frac{\Delta y_j}{2}\eta_0, \qquad \eta_0 \in [-1,1], \qquad j = 1,2,\cdots,N_y, \tag{4.3}$$

with $\tilde{y}_0 = \tilde{y}_{N_y} - 1$. The P-mesh and Q-mesh are used for the auxiliary variables p and q, respectively. Similar to the problem in one space dimension, we can also define $P_{\frac{1}{2},j} = ([0,\tilde{x}_1]\cup[\tilde{x}_{N_x},1])\times J_j$ and $Q_{j,\frac{1}{2}} = I_i \times ([0,\tilde{y}_1]\cup[\tilde{y}_{N_y},1])$.

We define the finite element spaces to be

$$\begin{aligned}
V_h &:= \{u_h : u_h|_{I_{ij}} \in Q^k(I_{ij}),\ i = 1,\cdots,N_x,\ j = 1,\cdots,N_y\}, \\
P_h &:= \{p_h : p_h|_{P_{i+\frac{1}{2},j}} \in Q^k(P_{i+\frac{1}{2},j}),\ i = 1,\cdots,N_x,\ j = 1,\cdots,N_y\}, \\
Q_h &:= \{q_h : q_h|_{Q_{i,j+\frac{1}{2}}} \in Q^k(Q_{i,j+\frac{1}{2}}),\ i = 1,\cdots,N_x,\ j = 1,\cdots,N_y\},
\end{aligned}$$

where Q^k is the tensor product polynomials of degree k. Given $u \in V_h$, we denote $u^+_{i-\frac{1}{2},j}$, $u^-_{i+\frac{1}{2},j}$, $u^+_{i,j-\frac{1}{2}}$, $u^-_{i,j+\frac{1}{2}}$ to be the traces of u on the four edges of I_{ij}, respectively. Likewise for the traces of $P_{i+\frac{1}{2},j}$ and $Q_{i,j+\frac{1}{2}}$ along $x = \tilde{x}_i$, $x = \tilde{x}_{i+1}$ and $y = \tilde{y}_j$, $y = \tilde{y}_{j+1}$, respectively. Moreover, we use $[u] = u^+ - u^-$ and $\{u\} = \frac{1}{2}(u^+ + u^-)$ as the jump and average of u at the cell interfaces, respectively.

Now, we can introduce the LDG method on the overlapping meshes: to find $(u_h, p_h, q_h) \in V_h \times P_h \times Q_h$, such that for any test functions $(v, w, z) \in V_h \times P_h \times Q_h$, we have

$$\begin{aligned}\int_{I_{ij}} (u_h)_t v dxdy = &- \int_{I_{ij}} a(u_h) p_h v_x dxdy + \int_{J_j} \hat{a}_{i+\frac{1}{2},j} \hat{p}_{i+\frac{1}{2},j} v^-_{i+\frac{1}{2},j} dy - \int_{J_j} \hat{a}_{i-\frac{1}{2},j} \hat{p}_{i-\frac{1}{2},j} v^+_{i-\frac{1}{2},j} dy, \\ &- \int_{I_{ij}} b(u_h) q_h v_y dxdy + \int_{I_i} \hat{b}_{i,j+\frac{1}{2}} \hat{q}_{i,j+\frac{1}{2}} v^-_{i,j+\frac{1}{2}} dx - \int_{I_i} \hat{b}_{i,j-\frac{1}{2}} \hat{q}_{i,j-\frac{1}{2}} v^+_{i,j-\frac{1}{2}} dx, \end{aligned} \tag{4.4}$$

$$\int_{P_{i+\frac{1}{2},j}} p_h w dxdy = - \int_{P_{i+\frac{1}{2},j}} A(u_h) w_x dxdy + \int_{J_j} A(u_h(\tilde{x}_{i+1})) w^-_{i+1,j} dy - \int_{J_j} A(u_h(\tilde{x}_i)) w^+_{i,j} dy, \tag{4.5}$$

$$\int_{Q_{i,j+\frac{1}{2}}} q_h z dxdy = - \int_{Q_{i,j+\frac{1}{2}}} B(u_h) z_y dxdy + \int_{I_i} B(u_h(\tilde{y}_{j+1})) z^-_{i,j+1} dx - \int_{I_i} B(u_h(\tilde{y}_j)) z^+_{i,j} dx. \tag{4.6}$$

The numerical flux $\hat{a}$ along $x = x_{i+\frac{1}{2}}$ and $\hat{b}$ along $y = y_{j+\frac{1}{2}}$ are taken as

$$\hat{a}_{i+\frac{1}{2},j} = \frac{[A(u_h)]_{i+\frac{1}{2},j}}{[u_h]_{i+\frac{1}{2},j}}, \quad \hat{b}_{i,j+\frac{1}{2}} = \frac{[B(u_h)]_{i,j+\frac{1}{2}}}{[u_h]_{i,j+\frac{1}{2}}},$$

where $[s]_{i+\frac{1}{2},j} := s^+_{i+\frac{1}{2},j} - s^-_{i+\frac{1}{2},j}$ denotes the jump of a function s across the cell boundary $\{x_{i+\frac{1}{2}}\} \times J_j$. Likewise for $[s]_{i,j+\frac{1}{2}}$. Moreover, we choose

$$\hat{p}_{i+\frac{1}{2},j} = p_h(x_{i+\frac{1}{2}}, y) + \frac{\alpha_{i+\frac{1}{2},j}}{\Delta\tilde{x}_{i+\frac{1}{2},j}} [u_h]_{i+\frac{1}{2},j}, \quad \hat{q}_{i,j+\frac{1}{2}} = q_h(x, y_{j+\frac{1}{2}}) + \frac{\alpha_{i,j+\frac{1}{2}}}{\Delta\tilde{x}_{i,j+\frac{1}{2}}} [u_h]_{i,j+\frac{1}{2}}.$$

To approximate the integral on I_i and J_j in (4.4)–(4.6), we use the three-point Gaussian quadrature. For each $\gamma = 1, 2, 3$, we can construct a quadratic polynomial $\psi^\gamma(x)$ in J_j such that

$$\begin{cases} \psi^\gamma(y^j_\sigma) = 1, \ \sigma = \gamma, \\ \psi^\gamma(y^j_\sigma) = 0, \ \sigma \neq \gamma, \end{cases}$$

where y^j_σ, $\sigma = 1, 2, 3$ are the three quadrature points in the Gaussian quadrature for J_j. Likewise for x^i_σ. In (4.5), we take $w(x, y) = \psi^\gamma(y)\tilde{w}(x)$, where $\tilde{w}(x)$ is a quadratic polynomial on $P_{i+\frac{1}{2}}$, to obtain

$$\int_{P_{i+\frac{1}{2}}} p_h(\cdot, y^j_\gamma) \tilde{w} dx = - \int_{P_{i+\frac{1}{2}}} A(u_h(\cdot, y^j_\gamma)) \tilde{w}_x dx + A(u_h(\tilde{x}_{i+1}, y^j_\gamma)) \tilde{w}^-_{i+1} - A(u_h(\tilde{x}_i, y^j_\gamma)) \tilde{w}^+_i, \tag{4.7}$$

which is similar to (2.3) and we can follow the same analyses in Section 3.2 to construct the MPP technique of problems in two space dimensions. Therefore, we only demonstrate the algorithm as follows and omit the proof.

1. Step 1: Modify $A(u_h)$ and $B(u_h)$. We only demonstrate how to modify $A(u_h)$ along the line segment $I = I_i \times \{y^j_\gamma\}$ and the procedure can be applied to $B(u_h)$ with minor changes. WLOG, we assume $m \le u \le M$.
   (a) Calculate a quadratic polynomial $p_2 \in P^2(I)$ such that p_2 is the interpolation of $A(u_h)$ at $x = x_{i-\frac{1}{2}}$, $x = x_i$, $x = x_{i+\frac{1}{2}}$ along I.
   (b) Compute a linear function $p_1 \in P^1(I)$ such that p_1 is the interpolation of $A(u_h)$ at $x = x_{i-\frac{1}{2}}$ and $x = x_{i+\frac{1}{2}}$ along I.
   (c) Apply a limiter to p_2: $\tilde{p} = \theta p_2 + (1-\theta) p_1$.
   (d) Choose the largest possible $\theta \in [0, 1]$ such that $\int_0^m a(u)\, du \le \tilde{p} \le \int_0^M a(u)\, du$, and use $\tilde{p}$ as $\tilde{A}$.
2. Step 2: Compute $p_h(x_{i+\frac{1}{2}}, y_\gamma)$. We use $\tilde{A}$ to replace A in (4.7) to obtain

$$\int_{P_{i+\frac{1}{2}}} p_h(\cdot, y^j_\gamma) \tilde{w} dx = - \int_{P_{i+\frac{1}{2}}} \tilde{A}(u_h(\cdot, y^j_\gamma)) \tilde{w}_x dx + \tilde{A}(\tilde{x}_{i+1}, y^j_\gamma) \tilde{w}^-_{i+1} - \tilde{A}(\tilde{x}_i, y^j_\gamma) \tilde{w}^+_i,$$

   and take suitable test function $\tilde{w}$ to obtain $p_h(x_{i+\frac{1}{2}}, y^j_\gamma)$. One example is (3.10).

3. Step 3: Update u_h in (4.4). We use the values of $p_h(x_{i+\frac{1}{2}}, y_\gamma^j)$ and $q_h(x_\gamma^i, y_{j+\frac{1}{2}})$ and three-point Gaussian quadrature to approximate the integrals on the cell interfaces. Following Lemma 3.5, we take

$$\frac{26\sqrt{6}}{27} - \frac{29}{9} \le \xi_0, \eta_0 \le \frac{29}{9} - \frac{26\sqrt{6}}{27},$$

and

$$\alpha_{i-\frac{1}{2},j} \ge \max\left\{g(1/dx_{i-\frac{1}{2}}, -\xi_0), g(dx_{i-\frac{1}{2}}, \xi_0)\right\},\ \alpha_{i,j-\frac{1}{2}} \ge \max\left\{g(1/dy_{j-\frac{1}{2}}, -\eta_0), g(dy_{j-\frac{1}{2}}, \eta_0)\right\},$$

where

$$dx_{i-\frac{1}{2}} = \frac{\Delta x_{i-1}}{\Delta x_i}, \quad dy_{j-\frac{1}{2}} = \frac{\Delta y_{j-1}}{\Delta y_j}.$$

Moreover, following Lemma 3.6, we also need to choose

$$\triangle t \le \frac{\mu_2 \triangle x^2}{12\mu_1 \tilde{C} \max_u a^2(u)\left[\max_i h(|\xi_{i+\frac{1}{2}}|) + 3\ell(\xi_0) + 3\max_{i,j}\alpha_{i+\frac{1}{2},j}\right]},$$

and

$$\triangle t \le \frac{\mu_2 \triangle y^2}{12\mu_1 \tilde{C} \max_u b^2(u)\left[\max_i h(|\eta_{i+\frac{1}{2}}|) + 3\ell(\eta_0) + 3\max_{i,j}\alpha_{i,j+\frac{1}{2}}\right]},$$

then we can obtain $m \le \bar{u}_h^{n+1} \le M$.

4. Step 4: Apply the bound-preserving limiter.
   (a) Set up a small number $\epsilon = 10^{-13}$.
   (b) If $\bar{u}_h \le m + \epsilon$ or $\bar{u}_h \ge M - \epsilon$, take $u_h = \bar{u}_h$. Then skip the following steps.
   (c) Define

$$m_{i,j}^x = \min_{x\in I_i, \gamma=1,2,3} u_h(x, y_\gamma^j), \quad M_{i,j}^x = \max_{x\in I_i, \gamma=1,2,3} u_h(x, y_\gamma^j).$$

   We can also define $m_{i,j}^y$ and $M_{i,j}^y$ analogously. Let

$$m_{i,j} = \min\{m_{i,j}^x, m_{i,j}^y\}, \quad M_{i,j} = \max\{M_{i,j}^x, M_{i,j}^y\},$$

   and set $\theta = 1$. If $m_{i,j} < m$ or $M_{i,j} > M$, then we take

$$\theta = \max\left\{\frac{\bar{u}_h - m - \epsilon}{\bar{u}_h - m_{i,j}}, \frac{\bar{u}_h - M + \epsilon}{\bar{u}_h - M_{i,j}}\right\}.$$

   (d) Compute $\tilde{u}_h = \bar{u}_h + \theta(u_h - \bar{u}_h)$, and use $\tilde{u}_h$ as the new numerical approximation.

Before, we finish this section, we would like to demonstrate the following remarks.

Remark 4.1. In step 1, we use $\tilde{A}$ to replace $A(u_h)$ along $I_i \times \{y_\gamma^j\}$. We can also extend $\tilde{A}$ to the whole cell $I_{i,j}$ such that $\tilde{A} \in V_h$, and use the new $\tilde{A}$ as A in (4.5) to compute the integrals exactly.

Remark 4.2. For linear equations, we can take piecewise P^k polynomials as the finite element space. In this case, $\hat{a}$ is a constant, hence we only need to evaluate $\int_{J_j} p(u_h)\, dy$ instead of p_h at the quadrature points. Therefore, in (4.5), we can take w as a function of x only to evaluate $\int_{J_j} p(u_h)\, dy$.

Remark 4.3. Due to the nature of overlapping meshes, it is not easy to extend the scheme to unstructured meshes. The technique for triangular meshes will be discussed in the future.

Table 5.1
Accuracy test for the linear heat equation.

Number of cells	LDG without limiter				LDG with limiter			
	L^2 norm	order	L^∞ norm	order	L^2 norm	order	L^∞ norm	order
	$\xi_0 = 0$							
10	3.05E-04	–	8.61E-04	–	2.33E-04	–	5.91E-04	–
20	3.85E-05	2.99	1.11E-04	2.95	2.84E-05	3.04	7.41E-05	2.99
40	4.83E-06	3.00	1.40E-05	2.99	3.52E-06	3.01	9.28E-06	3.00
80	6.04E-07	3.00	1.75E-06	3.00	4.39E-07	3.00	1.16E-06	3.00
160	7.55E-08	3.00	2.19E-07	3.00	5.49E-08	3.00	1.45E-07	3.00
320	9.43E-09	3.00	2.74E-08	3.00	6.86E-09	3.00	1.81E-08	3.00
	$\xi_0 = \sqrt{3}/3$							
10	3.09E-04	–	1.03E-03	–	2.40E-04	–	7.63E-04	–
20	3.76E-05	3.04	1.26E-04	3.03	2.98E-05	3.01	9.62E-05	2.99
40	4.67E-06	3.01	1.57E-05	3.01	3.73E-06	3.00	1.20E-05	3.00
80	5.83E-07	3.00	1.96E-06	3.00	4.66E-07	3.00	1.51E-06	3.00
160	7.28E-08	3.00	2.44E-07	3.00	5.82E-08	3.00	1.88E-07	3.00
320	9.10E-09	3.00	3.05E-08	3.00	7.28E-09	3.00	2.35E-08	3.00

Table 5.2
Accuracy test for the nonlinear heat equation.

Number of cells	LDG without limiter				LDG with limiter			
	L^2 norm	order	L^∞ norm	order	L^2 norm	order	L^∞ norm	order
	$\xi_0 = 0$							
10	2.32E-04	–	8.31E-04	–	1.84E-04	–	5.92E-04	–
20	2.93E-05	2.99	1.04E-04	2.99	2.22E-05	3.05	7.41E-05	3.00
40	3.67E-06	3.00	1.32E-05	2.98	2.75E-06	3.01	9.25E-06	3.00
80	4.59E-07	3.00	1.65E-06	3.00	3.43E-07	3.00	1.15E-06	3.00
160	5.74E-08	3.00	2.06E-07	3.00	4.29E-08	3.00	1.44E-07	3.00
320	7.20E-09	2.99	2.62E-08	2.98	5.36E-09	3.00	1.80E-08	3.00
	$\xi_0 = \sqrt{3}/3$							
10	2.38E-04	–	9.79E-04	–	1.88E-04	–	7.32E-04	–
20	2.88E-05	3.04	1.19E-04	3.05	2.33E-05	3.01	9.31E-05	2.97
40	3.57E-06	3.01	1.48E-05	3.01	2.91E-06	3.00	1.16E-05	3.00
80	4.46E-07	3.00	1.84E-06	3.00	3.64E-07	3.00	1.45E-06	3.00
160	5.57E-08	3.00	2.30E-07	3.00	4.54E-08	3.00	1.82E-07	3.00
320	6.96E-09	3.00	2.89E-08	3.00	5.68E-09	3.00	2.27E-08	3.00

5. Numerical examples

In this section, we provide numerical experiments to demonstrate the performance of the third-order MPP LDG method. For simplicity, uniform primitive meshes ($dx_{i+\frac{1}{2}} = 1$ for all i) are used in all numerical examples. In this case, all penalty parameters $\alpha_{i+\frac{1}{2}}$ at different cell boundaries are in fact the same and hence we simply rewrite it as α. We test different offsets of the auxiliary mesh in each numerical example. For $\xi_0 = 0$, we take the penalty parameter as $\alpha = 0.42$, and for $\xi_0 = \sqrt{3}/3$, we take $\alpha = 0.25$. For simplicity, we only test the preserving property of the lower bound of the solution. The results for preserving the upper bound are similar. Hence, we take $M = \infty$. We use the third-order TVD Runge–Kutta method for time discretization and the third-order LDG scheme on overlapping meshes for the space discretization.

5.1. One-dimensional numerical tests

Example 5.1. We consider the following linear heat equation

$$\begin{cases} u_t = u_{xx}, \\ u(x,0) = \sin(x) + 1, \end{cases} \tag{5.1}$$

on $[0, 2\pi]$ with a 2π-periodic boundary condition.

The exact solution is $u(x,t) = e^{-t}\sin(x) + 1$. Numerical errors at $T = 1$ with different values of ξ_0 are listed in Table 5.1. In the left column, we test the LDG method without limiter. That is, we take $\alpha = 0$ and do not apply the slope limiter described on Page 15. We can observe the expected third-order accuracy for our scheme on overlapping meshes. In the right column of the table, we take $m = 0$ and apply the PP limiter. Here only the solutions on the two elements sharing

Table 5.3
Accuracy test for the linear convection-diffusion equation.

Number of cells	LDG without limiter				LDG with limiter			
	L^2 norm	order	L^∞ norm	order	L^2 norm	order	L^∞ norm	order
	$\xi_0 = 0$							
10	8.56E-04	–	2.59E-03	–	8.99E-04	–	3.14E-03	–
20	1.06E-04	3.01	3.12E-04	3.05	1.07E-04	3.08	3.12E-04	3.33
40	1.32E-05	3.01	3.90E-05	3.00	1.32E-05	3.01	3.91E-05	3.00
80	1.63E-06	3.02	4.78E-06	3.03	1.64E-06	3.01	4.81E-06	3.02
160	1.99E-07	3.04	5.74E-07	3.06	2.01E-07	3.03	5.81E-07	3.05
320	2.37E-08	3.07	6.63E-08	3.11	2.42E-08	3.05	6.79E-08	3.10
	$\xi_0 = \sqrt{3}/3$							
10	8.56E-04	–	2.59E-03	–	8.97E-04	–	3.11E-03	–
20	1.06E-04	3.01	3.11E-04	3.06	1.06E-04	3.08	3.12E-04	3.32
40	1.32E-05	3.01	3.88E-05	3.01	1.32E-05	3.01	3.88E-05	3.00
80	1.63E-06	3.02	4.73E-06	3.03	1.63E-06	3.02	4.75E-06	3.03
160	1.98E-07	3.04	5.64E-07	3.07	2.00E-07	3.03	5.68E-07	3.06
320	2.37E-08	3.06	6.46E-08	3.13	2.40E-08	3.06	6.53E-08	3.12

Table 5.4
Elements that have been modified by the slope limiter.

Time	Cell	Time	Cell	Time	Cell
$N_x = 10$		$N_x = 20$		$N_x = 40$	
3.95E-02	8	0	15, 16	0	30, 31
7.90E-02	8	9.87E-03	16	2.47E-03	31
1.18E-01	8	1.97E-02	16		
1.58E-01	8	2.96E-02	16		
1.97E-01	8				
2.37E-01	8				
2.76E-01	8, 9				
3.16E-01	8, 9				
3.55E-01	9				
3.95E-01	9				
9.47E-01	10				
$N_x = 80$		$N_x = 160$		$N_x = 320$	
0	60, 61	0	120, 121	0	240, 241

the minimum value point $x = \frac{3}{2}\pi$ are modified by the slope limiter at the initial time. But the authors in [28] have already proved that this slope limiter keeps the high-order accuracy. In our test, we take $\alpha \neq 0$ in all cells even though most of them do not need to apply the PP limiter. We can observe that the penalty term with $\alpha \neq 0$ indeed does not harm the original high order accuracy.

Example 5.2. We consider the following nonlinear heat equation

$$\begin{cases} u_t = (e^{0.2u} u_x)_x, \\ u(x,0) = \sin(x) + 1, \end{cases} \tag{5.2}$$

on $[0, 2\pi]$ with a 2π-periodic boundary condition.

For this nonlinear problem, the exact solution is not easy to derive. However, when computing the numerical error for N cells, we can treat the numerical solution with $2N$ cells as the reference solution. Numerical errors at $T = 1$ are listed in Table 5.2. We can also observe the expected third-order accuracy for our scheme on overlapping meshes. In this example, we take $m = 0$. As in the previous example, the slope limiter only works on the two elements sharing the point $x = \frac{3}{2}\pi$ at the initial time. However, we still take $\alpha \neq 0$ and replace A by $\tilde{A}$ in all cells at all time levels. By comparing the left and right columns of the error table, we can observe that the penalty term in our scheme and the replacement of A by $\tilde{A}$ will not harm the original third-order of accuracy of the LDG method.

Example 5.3. We consider the following linear convection-diffusion equation

$$\begin{cases} u_t + u_x = \epsilon u_{xx}, \\ u(x,0) = \sin(x), \end{cases} \tag{5.3}$$

on $[0, 2\pi]$ with a 2π-periodic boundary condition.

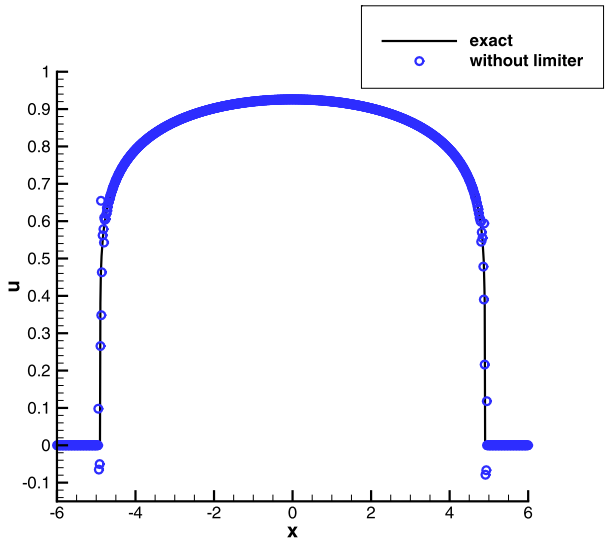

(a) $\xi_0 = 0$ without limiter

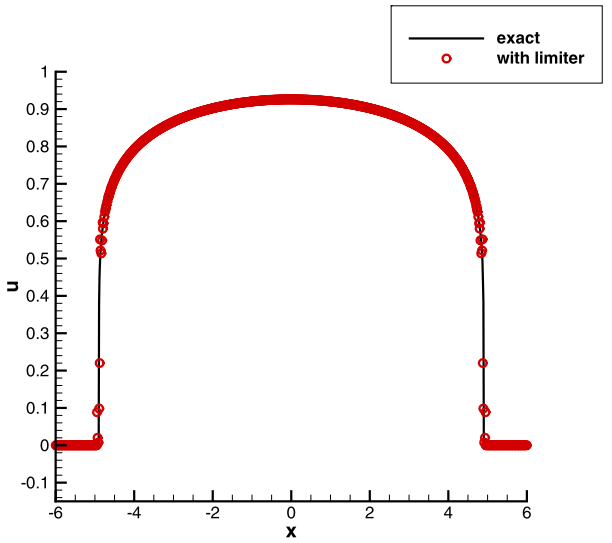

(b) $\xi_0 = 0$ with limiter

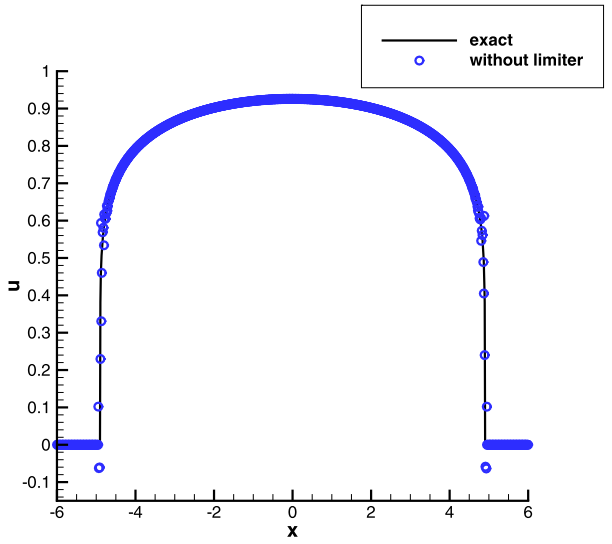

(c) $\xi_0 = \sqrt{3}/3$ without limiter

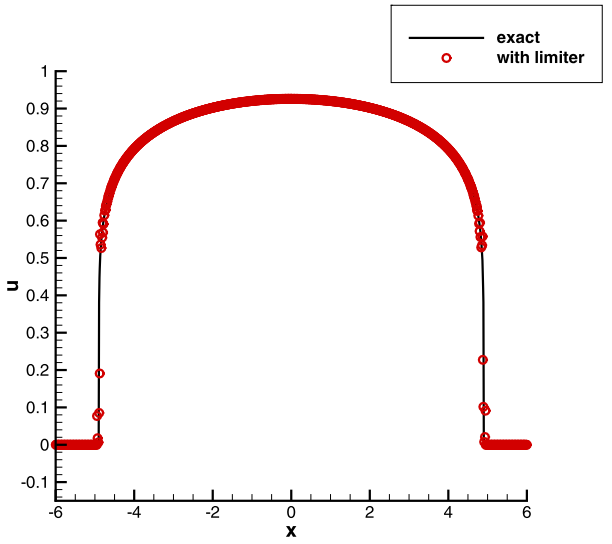

(d) $\xi_0 = \sqrt{3}/3$ with limiter

Fig. 5.1. Porous medium equation with $m = 8$. Comparison of numerical solutions with and without limiters.

The exact solution is $u(x,t) = exp(-\epsilon t)sin(x-t)$. We take $\epsilon = 0.001$. Numerical errors at $T = 1$ are listed in Table 5.3. In the MPP limiter, we take $m = -1$. In Table 5.4, we list the indices of cells that have been modified by the slope limiter with $\xi_0 = 0$. The results for $\xi_0 = \sqrt{3}/3$ are exactly the same. We can see that the slope limiter works on the elements containing the global minimum at several time levels. We still take $\alpha \neq 0$ globally at each time level and can also observe the expected third-order accuracy for the MPP LDG scheme. Therefore, the technique also works for convection-diffusion equations.

Example 5.4. We consider the following porous medium equation

$$u_t = (u^m)_{xx}, \qquad m > 1. \tag{5.4}$$

This is a classical example of degenerate parabolic equations. We use the Barenblatt solution

$$B_m(x,t) = t^{-k}\left[\left(1 - \frac{k(m-1)}{2m}\frac{|x|^2}{t^{2k}}\right)_+\right]^{\frac{1}{m-1}}, \tag{5.5}$$

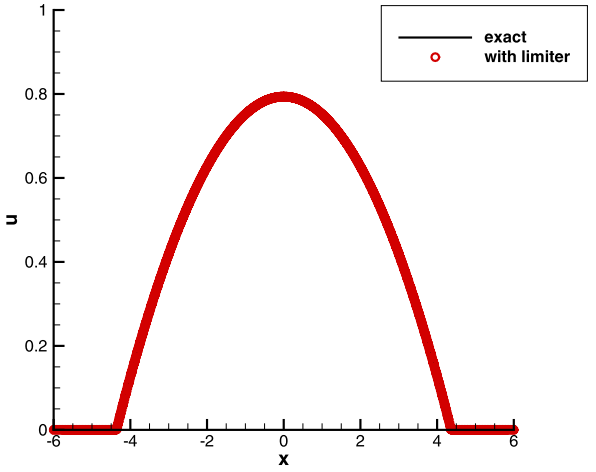

(a) $\xi_0 = 0$, $m = 2$

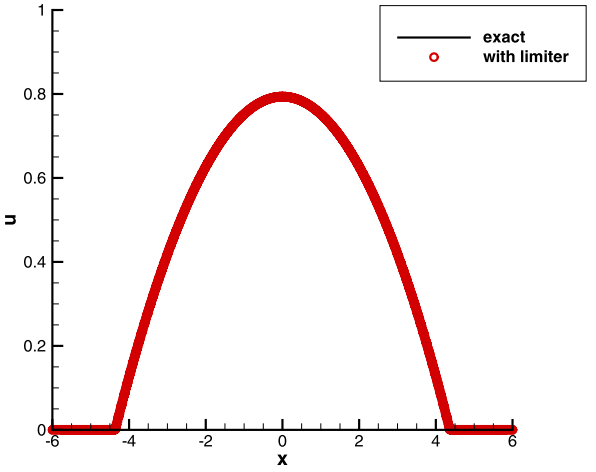

(b) $\xi_0 = \sqrt{3}/3$, $m = 2$

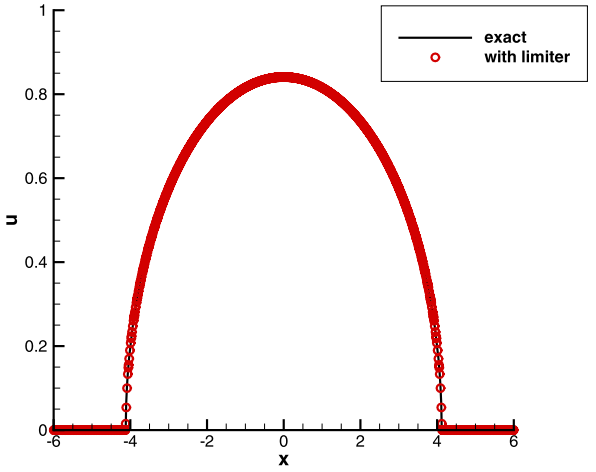

(c) $\xi_0 = 0$, $m = 3$

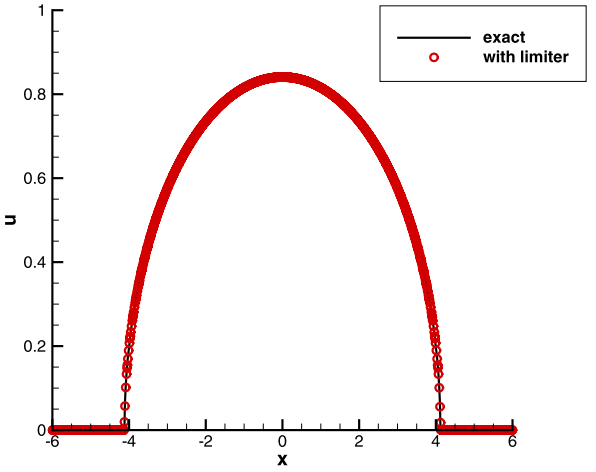

(d) $\xi_0 = \sqrt{3}/3$, $m = 3$

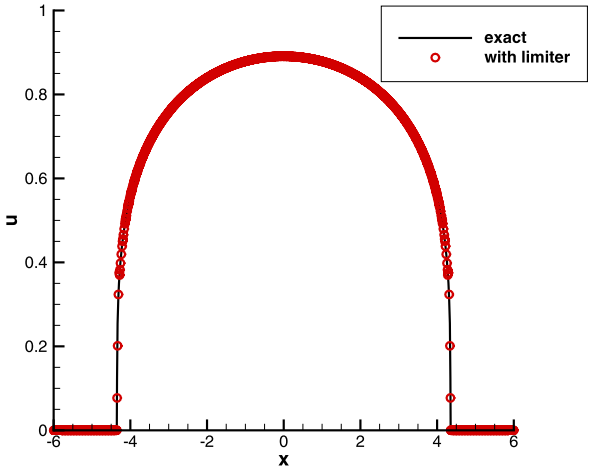

(e) $\xi_0 = 0$, $m = 5$

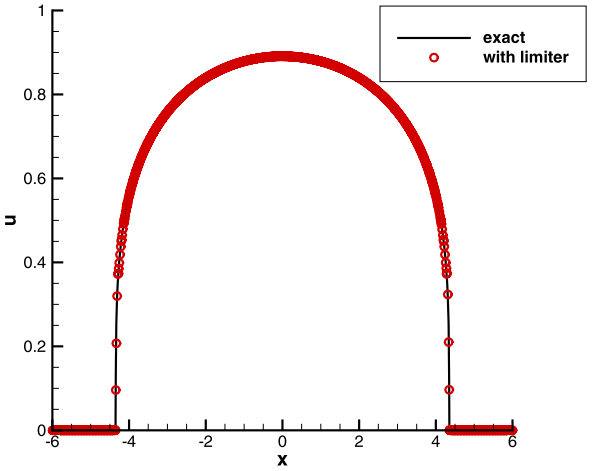

(f) $\xi_0 = \sqrt{3}/3$, $m = 5$

Fig. 5.2. Porous medium equation with limiter. Different m.

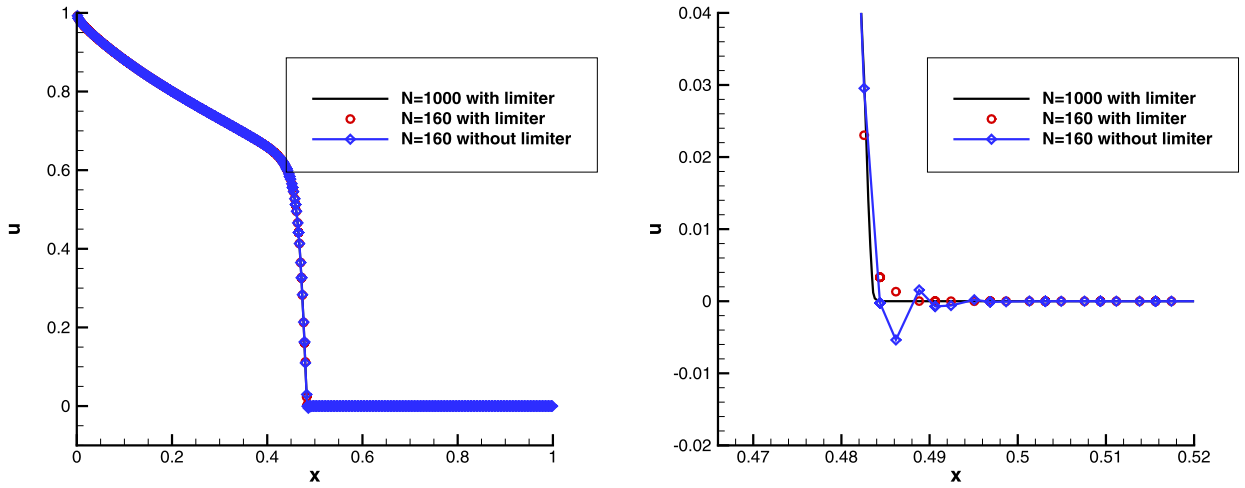

(a) Solutions computed with and without limiter

(b) Zoom in results near the corner of the solutions

Fig. 5.3. Buckley–Leverett equation. $\xi_0 = 0$.

Table 5.5
Accuracy test for the linear convection-diffusion equation in 2D.

Number of cells	LDG without limiter				LDG with limiter			
	L^2 norm	order	L^∞ norm	order	L^2 norm	order	L^∞ norm	order
	$\xi_0 = 0$							
10	8.68E-04	–	1.83E-03	–	8.68E-04	–	1.83E-03	–
20	1.15E-04	2.92	2.54E-04	2.85	1.15E-04	2.92	2.54E-04	2.85
40	1.42E-05	3.01	3.18E-05	3.00	1.43E-05	3.01	3.19E-05	3.00
80	1.76E-06	3.02	3.92E-06	3.02	1.77E-06	3.02	3.95E-06	3.01
160	2.14E-07	3.04	4.77E-07	3.04	2.16E-07	3.03	4.84E-07	3.03
320	2.52E-08	3.08	5.63E-08	3.08	2.59E-08	3.06	5.79E-08	3.06
	$\xi_0 = \sqrt{3}/3$							
10	8.68E-04	–	1.83E-03	–	8.68E-04	–	1.83E-03	–
20	1.15E-04	2.92	2.54E-04	2.85	1.15E-04	2.92	2.54E-04	2.85
40	1.42E-05	3.01	3.17E-05	3.00	1.43E-05	3.01	3.18E-05	3.00
80	1.75E-06	3.02	3.91E-06	3.02	1.76E-06	3.02	3.93E-06	3.02
160	2.13E-07	3.04	4.75E-07	3.04	2.14E-07	3.04	4.79E-07	3.04
320	2.52E-08	3.08	5.60E-08	3.08	2.56E-08	3.07	5.69E-08	3.07

where $k = \frac{1}{m+1}$. This is an exact solution to the porous medium equation in one space dimension with compact support. The initial condition is taken to be $B_m(x, 1)$, and the numerical solution is computed to $T = 2$. We take $\xi_0 = 0$ with $\alpha = 0.42$, and $\xi_0 = \sqrt{3}/3$ with $\alpha = 0.25$, respectively.

In Fig. 5.1, we take $m = 8$ and compare the original numerical solutions without limiter and the numerical solutions with the MPP limiter. For the numerical solutions without limiter, we can see that there are significant undershoots near the foot of the solutions. While our MPP limiter keeps the solutions strictly non-negative in the whole computational domain. Fig. 5.2 shows the numerical solutions with limiter for different values of m. We can see that the MPP LDG scheme on overlapping meshes resolves the discontinuities in the solutions quite well and keeps the solution strictly non-negative.

Example 5.5. We consider the following convection-diffusion Buckley–Leverett equation, which is often used in reservoir simulations

$$u_t + f(u)_x = \epsilon(\nu(u)u_x)_x, \qquad x \in [0, 1],$$

where $f(u)$ and $\nu(u)$ are given as

$$f(u) = \frac{u^2}{u^2 + (1-u)^2}, \quad \nu(u) = \begin{cases} 4u(1-u), & 0 \leqslant u \leqslant 1, \\ 0, & \textit{otherwise}. \end{cases}$$

The initial and boundary conditions are given as

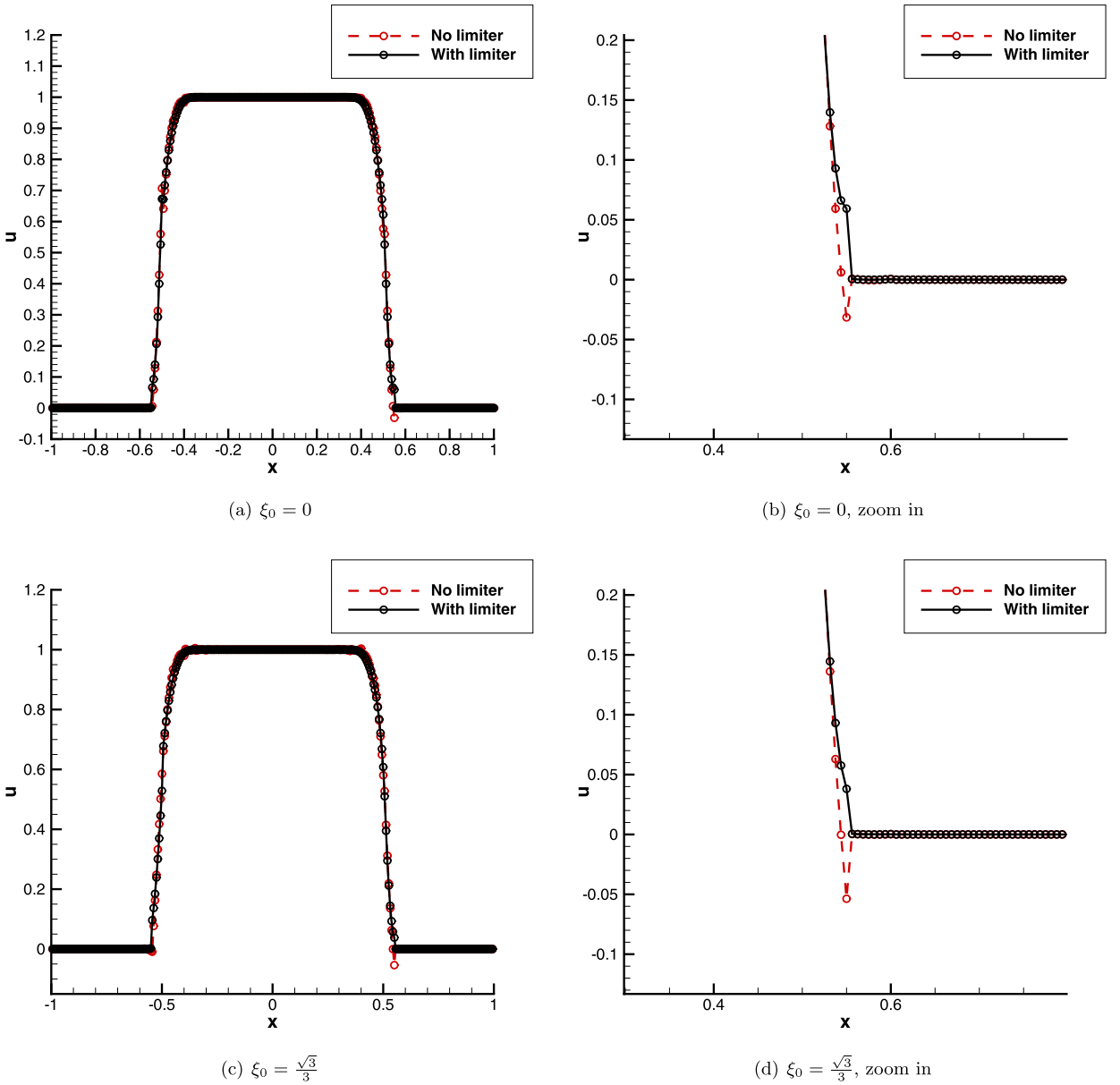

(a) $\xi_0 = 0$ (b) $\xi_0 = 0$, zoom in

(c) $\xi_0 = \frac{\sqrt{3}}{3}$ (d) $\xi_0 = \frac{\sqrt{3}}{3}$, zoom in

Fig. 5.4. Porous medium equation at $T = 0.0005$. $N = 40$.

$$u(x,0) = \begin{cases} 1 - 3x, & 0 \leqslant x \leqslant 1/3, \\ 0, & 1/3 \leqslant x \leqslant 1, \end{cases} \qquad u(0,t) = 1.$$

We take $\epsilon = 0.01$ and $\xi_0 = 0$ in our numerical test. Numerical solutions at $T = 0.2$ with and without limiter are shown in Fig. 5.3. For the solution computed without limiter, there are some undershoots near the foot of the solution. While our MPP limiter can eliminates all negative values. Numerical results for $\xi_0 = \sqrt{3}/3$ are similar, thus we will not show them here to save space.

5.2. Two-dimensional numerical tests

Example 5.6. We consider the following two-dimensional linear convection-diffusion equation

$$\begin{cases} u_t + \nabla \cdot u = \epsilon \triangle u, \\ u(x, y, 0) = \sin(2\pi (x + y)), \end{cases} \tag{5.6}$$

on $[0, 1] \times [0, 1]$ with periodic boundary conditions.

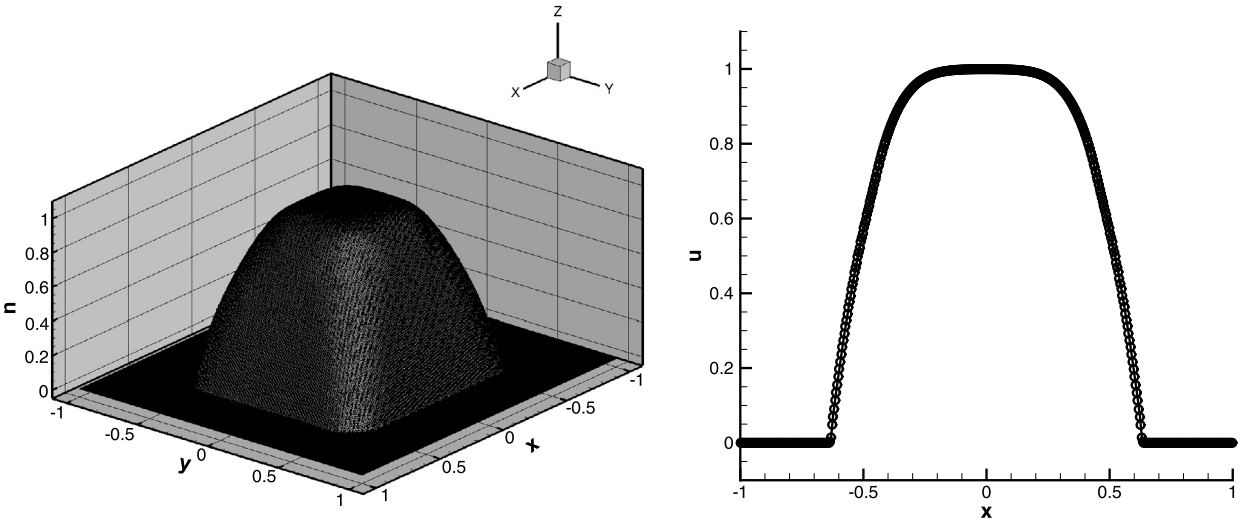

(a) surface of the solution (b) Cut along $y = 0$

Fig. 5.5. Porous medium equation at $T = 0.005$. LDG with maximum-principle-satisfying limiter. $\xi_0 = 0$, $N = 160$.

The exact solution is $u(x, y, t) = exp(-8\pi^2\epsilon t)sin(2\pi(x + y - 2t))$. We take $\epsilon = 0.0001$. Numerical errors at $T = 0.1$ are listed in Table 5.5. We observe the expected third-order rate of convergence. Also, the MPP limiter does not harm the original third-order accuracy.

Example 5.7. We test the two-dimensional porous medium equation

$$u_t = \triangle(u^2), \tag{5.7}$$

with a periodic boundary condition and the initial condition

$$u(x, y, 0) = \begin{cases} 1, & if\ (x, y) \in [-\frac{1}{2}, \frac{1}{2}] \times [-\frac{1}{2}, \frac{1}{2}], \\ 0, & otherwise, \end{cases} \tag{5.8}$$

in the computational domain $[-1, 1] \times [-1, 1]$.

Following [30], we compared MPP LDG scheme with the one without limiters at time $t = 0.0005$, as shown in Fig. 5.4. We can see that without the MPP technique, the scheme will yield non-physical negative values and the numerical approximations will blow up eventually, while the MPP limiter keeps the numerical solution nonnegative. Numerical results with MPP limiter at a later time $T = 0.005$ are shown in Fig. 5.5. Here we take $\xi_0 = 0$. Results for $\xi_0 = \sqrt{3}/3$ are similar. We can see that the numerical solution is nonnegative and the scheme is stable. Also, our scheme resolves the discontinuities in the solutions quite well.

6. Conclusion

In this paper, we have constructed third-order MPP LDG methods on overlapped meshes. The penalty in the scheme does not depend on the numerical approximation and tends to infinity if the dual mesh moves towards the primitive mesh. Numerical experiments demonstrated the good performance of the scheme.

References

[1] F. Bassi, S. Rebay, A high-order accurate discontinuous finite element method for the numerical solution of the compressible Navier–Stokes equations, J. Comput. Phys. 131 (1997) 267–279.
[2] Z. Chen, H. Huang, J. Yan, Third order maximum-principle-satisfying direct discontinuous Galerkin methods for time dependent convection diffusion equations on unstructured triangular meshes, J. Comput. Phys. 308 (2016) 198–217.
[3] E. Chung, C.S. Lee, A staggered discontinuous Galerkin method for the convection-diffusion equation, J. Numer. Math. 20 (2012) 1–31.
[4] B. Cockburn, S. Hou, C.-W. Shu, The Runge–Kutta local projection discontinuous Galerkin finite element method for conservation laws IV: the multidimensional case, Math. Comput. 54 (1990) 545–581.
[5] B. Cockburn, S.-Y. Lin, C.-W. Shu, TVB Runge–Kutta local projection discontinuous Galerkin finite element method for conservation laws III: one-dimensional systems, J. Comput. Phys. 84 (1989) 90–113.
[6] B. Cockburn, C.-W. Shu, TVB Runge–Kutta local projection discontinuous Galerkin finite element method for conservation laws II: general framework, Math. Comput. 52 (1989) 411–435.

[7] B. Cockburn, C.-W. Shu, The Runge–Kutta discontinuous Galerkin method for conservation laws V: multidimensional systems, J. Comput. Phys. 141 (1998) 199–224.
[8] B. Cockburn, C.-W. Shu, The local discontinuous Galerkin method for time dependent convection-diffusion systems, SIAM J. Numer. Anal. 35 (1998) 2440–2463.
[9] J. Douglas Jr., R.E. Ewing, M.F. Wheeler, A time-discretization procedure for a mixed finite element approximation of miscible displacement in porous media, RAIRO. Anal. Numér. 17 (1983) 249–256.
[10] J. Douglas Jr., R.E. Ewing, M.F. Wheeler, The approximation of the pressure by a mixed method in the simulation of miscible displacement, RAIRO. Anal. Numér. 17 (1983) 17–33.
[11] J. Du, Y. Yang, E. Chung, Local discontinuous Galerkin methods for convection-diffusion equations on overlapped meshes, submitted for publication.
[12] I.M. Gelfand, Some questions of analysis and differential equations, Am. Math. Soc. Trans. 26 (1963) 201–219.
[13] S. Gottlieb, C.-W. Shu, E. Tadmor, Strong stability-preserving high-order time discretization methods, SIAM Rev. 43 (2001) 89–112.
[14] H. Guo, Y. Yang, Bound-preserving discontinuous Galerkin method for compressible miscible displacement problem in porous media, SIAM J. Sci. Comput. 39 (2017) A1969–A1990.
[15] L. Guo, Y. Yang, Positivity-preserving high-order local discontinuous Galerkin method for parabolic equations with blow-up solutions, J. Comput. Phys. 289 (2015) 181–195.
[16] A.E. Hurd, D.H. Sattinger, Questions of existence and uniqueness for hyperbolic equations with discontinuous coefficients, Trans. Am. Math. Soc. 132 (1968) 159–174.
[17] E.F. Keller, L.A. Segel, Initiation on slime mold aggregation viewed as instability, J. Theor. Biol. 26 (1970) 399–415.
[18] X. Li, C.-W. Shu, Y. Yang, Local discontinuous Galerkin method for the Keller–Segel chemotaxis model, J. Sci. Comput. 73 (2017) 943–967.
[19] Y. Liu, C.-W. Shu, E. Tadmor, M. Zhang, Central local discontinuous Galerkin methods on overlapping cells for diffusion equations, ESAIM: Math. Model. Numer. Anal. (M2AN) 45 (2011) 1009–1032.
[20] C. Patlak, Random walk with persistence and external bias, Bull. Math. Biophys. 15 (1953) 311338.
[21] T. Qin, C.-W. Shu, Y. Yang, Bound-preserving discontinuous Galerkin methods for relativistic hydrodynamics, J. Comput. Phys. 315 (2016) 323–347.
[22] W.H. Reed, T.R. Hill, Triangular Mesh Methods for the Neutron Transport Equation, Los Alamos Scientific Laboratory Report LA-UR-73-479, Los Alamos, NM, 1973.
[23] C.-W. Shu, Total-variation-diminishing time discretizations, SIAM J. Sci. Stat. Comput. 9 (1988) 1073–1084.
[24] C.-W. Shu, S. Osher, Efficient implementation of essentially non-oscillatory shock-capturing schemes, J. Comput. Phys. 77 (1988) 439–471.
[25] T. Xiong, J.-M. Qiu, Z. Xu, High order maximum-principle-preserving discontinuous Galerkin method for convection-diffusion equations, SIAM J. Sci. Comput. 37 (2015) A583–A608.
[26] Y. Yang, D. Wei, C.-W. Shu, Discontinuous Galerkin method for Krause's consensus models and pressureless Euler equations, J. Comput. Phys. 252 (2013) 109–127.
[27] X. Zhang, C.-W. Shu, On maximum-principle-satisfying high order schemes for scalar conservation laws, J. Comput. Phys. 229 (2010) 3091–3120.
[28] X. Zhang, C.-W. Shu, On positivity preserving high order discontinuous Galerkin schemes for compressible Euler equations on rectangular meshes, J. Comput. Phys. 229 (2010) 8918–8934.
[29] X. Zhang, C.-W. Shu, Positivity-preserving high order discontinuous Galerkin schemes for compressible Euler equations with source terms, J. Comput. Phys. 230 (2011) 1238–1248.
[30] Y. Zhang, X. Zhang, C.-W. Shu, Maximum-principle-satisfying second order discontinuous Galerkin schemes for convection-diffusion equations on triangular meshes, J. Comput. Phys. 234 (2013) 295–316.
[31] X. Zhao, Y. Yang, C. Seyler, A positivity-preserving semi-implicit discontinuous Galerkin scheme for solving extended magnetohydrodynamics equations, J. Comput. Phys. 278 (2014) 400–415.